Direct and indirect Structural Health Monitoring of steel railway bridges: A state-of-the-art review and future challenges

Christos Sakaris[1], Zihao Liu[2], Mehrisadat Makki Alamdari[2] and Rune Schlanbusch[1]

[1] *DARWIN group, Energy and Technology Division, NORCE Research AS, 4879, Grimstad, Norway*
csak@norceresearch.no rusc@norceresearch.no

[2] *School of Civil and Environmental Engineering, University of New South Wales, Sydney, Australia*
zihao.liu8@unsw.edu.au m.makkialamdari@unsw.edu.au

ABSTRACT

Steel railway bridges are a vital part of the transportation infrastructure, and their normal operation is crucial to a functioning society. However, aging bridges are subjected to traffic loads and harsh environmental conditions, which can lead to deterioration mechanisms. When damages caused by such mechanisms reach a critical level, they can lead to catastrophic bridge failures, high maintenance costs, and loss of human lives. Thus, early damage detection, localization, quantification, and the estimation of the remaining useful life of a bridge are crucial. Structural Health Monitoring (SHM) systems based on vibration measurements have been developed for bridge monitoring. SHM is characterized as direct or indirect (drive-by) depending on how the sensors are used. In direct SHM, vibration sensors are mounted on the bridge to measure the response of the bridge as the trains pass, while in indirect SHM, vibration sensors are installed on passing trains to measure the response of the bridge. The high cost for the deployment and maintenance of direct SHM instrumentation across the large number of bridges in a typical railway network limits its scalability, making network-wide deployment economically impractical. As a result, indirect SHM has been explored as a less costly alternative for network-level monitoring, while direct SHM remains highly valuable for critical assets, high-risk structures, and validating indirect monitoring methods. Despite growing interest, the main research gap is the existence of only two review papers on SHM in steel railway bridges, with the studies referred to in the review papers covering only direct SHM and mainly damage detection, localization, and quantification. The goal of the current review article is to address this research gap by reviewing the state-of-the-art in SHM methods applied to steel railway bridges between 2010 and 2025. The state-of-the-art encompasses direct SHM studies with numerical, experimental, and field validation on full-scale bridges, and indirect SHM studies with numerical and field validation on full-scale bridges and experimental validation on laboratory-scaled bridges. Within indirect SHM, frequency identification, which recovers bridge natural frequencies from train-mounted sensors, is treated as an enabling monitoring task that supports SHM workflow. In addition, the review article provides recommendations for future challenges.

Christos Sakaris et al. This is an open-access article distributed under the terms of the Creative Commons Attribution 3.0 United States License, which permits unrestricted use, distribution, and reproduction in any medium, provided the original author and source are credited.

1. INTRODUCTION

The continuous operation of steel railway bridges, which form critical assets of the transportation infrastructure, is essential for the functioning of society. (Vagnoli, Remenyte-Prescott, & Andrews, 2017). However, bridge aging and harsh operational environmental conditions can trigger deterioration mechanisms, leading to damage (Frøseth & Rönnquist, 2019; Ghiasi, Ng, & Sheikh, 2022; Zakharenko, M., Frøseth, & Ronnquist, 2022; Svendsen, Oiseth, Froseth, & Ronnquist, 2023). Reaching critical severity of these damages can lead to catastrophic consequences, including bridge collapse, increased maintenance cost, and human casualties (Imam & Chryssanthopoulos, 2012; Ye, Su, & Han, 2014; Azim & Gul, 2021). Therefore, early diagnosis - encompassing damage detection, localization, and quantification (Svendsen et al., 2023)- together with damage prognosis through the estimation of the Remaining Useful Life (RUL) of a bridge (Frøseth & Rönnquist, 2019; Zakharenko et al., 2022), are crucial for effective maintenance planning, reducing maintenance cost, and preventing severe consequences.

Damage diagnosis and prognosis in steel railway bridges have been investigated through the deployment of Structural Health Monitoring (SHM) systems, which consist mainly of vibration sensors, data-acquisition systems, communication hardware, and analysis software for continuously or periodically assess-

ing the integrity of the bridges (Vagnoli et al., 2017). Thus, these SHM systems operate based on vibration measurements, resulting in reduced monitoring / assessment costs and continuous availability of SHM data. The concept of the vibration-based SHM methods is that damage alters the stiffness or mass of the examined structure, which, in turn, alters the structure's measured global dynamic response properties, and damage diagnosis is achieved via the examination of changes in the structure's vibration characteristics (Ye et al., 2014; Vagnoli et al., 2017). The variability of Operational and Environmental Conditions (EOCs) hinders SHM's effectiveness as EOCs partially or fully "mask" the effects of damage on structural dynamics.

Depending on how the sensors are used, SHM is characterized as direct or indirect (drive-by). In direct SHM, the responses of the bridges vibrated by the passing train are measured via vibration sensors, which are mounted on the bridges, while in indirect SHM, the responses of the bridges are measured via vibration sensors installed on various parts of the passing trains (Bernardini, Carnevale, & Collina, 2021; Bernardini, Bono, & Collina, 2025b). The mass deployment of direct SHM systems and the maintenance of the instrumentation across a large number of unmonitored bridges represents a high and prohibitive cost with limited scalability, thus making network-wide direct SHM economically impractical rather than technically infeasible. Due to these disadvantages, the indirect SHM approach and bridge monitoring via trains acting as mobile sensors to detect damages have been explored as a less costly alternative (Bernardini et al., 2021, 2025b). However, the indirect approach faces challenges, including sensitivity to train–track–bridge interaction, environmental and operational variability, and the need for robust domain adaptation and generalization. Direct SHM retains clear value for individual critical or high-risk bridges, where the cost of permanent instrumentation is justified by the structural importance of the asset and the need for high-resolution condition assessment. It is precisely this complementarity, network-level monitoring via indirect SHM and targeted high-resolution assessment via direct SHM, that would motivate a combined deployment strategy.

The state-of-the-art on direct and indirect SHM in steel railway bridges shows that the direct SHM approach has been researched more extensively than the indirect SHM approach. The review of the state-of-the-art is based on studies published between 2010 and 2025, considering direct SHM studies with numerical and experimental validation on full-scale bridges, and field validation, and indirect SHM studies with numerical validation on full-scale bridges, experimental validation on laboratory-scaled bridges, and field validation. A systematic approach has been employed for screening the studies, using defined search criteria, specific search keywords, and a selection process (see Table 1). Based on this approach, the state-of-the-art has been refined to include 32 studies about direct SHM, and 13 studies about indirect SHM, of which 6 focus on frequency identification and 7 on damage diagnosis.

According to Fig. 1, which presents the number of annual studies published from 2010 to 2025, the publications about indirect SHM appear since 2019, whereas the total numbers of reviewed studies about direct and indirect SHM are 32 and 13, respectively, with the 13 indirect SHM studies comprising 6 frequency identification studies and 7 damage diagnosis studies. These studies have been published in 20 journals and five conference proceedings, as shown in Table 2, and have been contributed by 20 countries, as shown in Fig. 2, with Italy making the highest contribution. Six types of bridges have been investigated in the reviewed studies, and they are mentioned in Fig. 3.

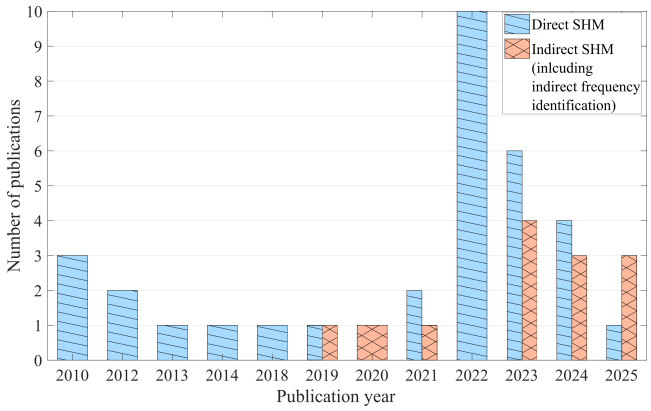

Figure 1. Distribution of direct and indirect SHM publications according to year.

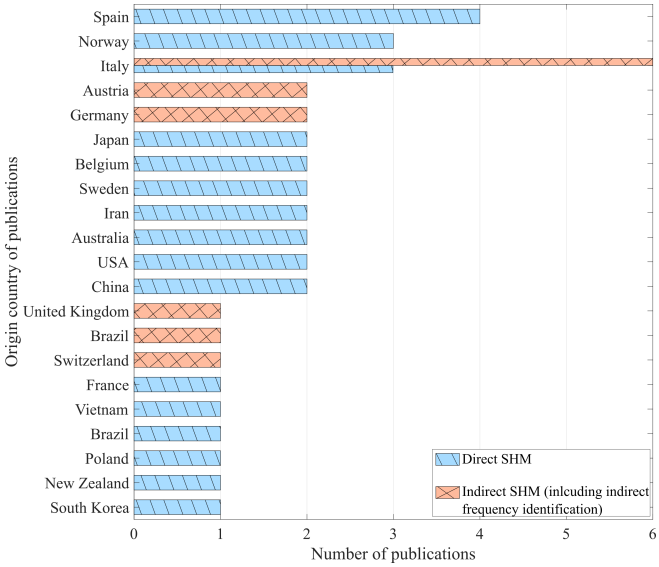

Figure 2. Distribution of direct and indirect SHM publications according to origin countries.

Regarding related review studies, only two exist (Vagnoli et al., 2017; Wang, Ni, & Wang, 2022), and they provide insights

Table 1. Approach for screening and selecting studies.

Searching index	**Specific content**
Scientific database	Scopus and Google Scholar
Article type	Scientific/technical articles published in peer-reviewed journals and conferences
Search keywords	”steel”, “railway bridge”,“train bridge”, train, bridge, “fault”, “damage”, “diagnosis”, ”monitoring”, ”Structural Health Monitoring”, “detection”, ”identification”, ”localization”, ”quantification”, ”prognosis”, ”remaining useful life”, ”reliability”, ”frequency identification”, ”drive-by”
Search strings	The operators AND, OR are used with the search keywords covering all the possible search strings
Search period	Between January 2010 and December 2025
Screening procedure	Relativity of each researched study is determined based on the study’s main text.
Selection process	The selection of studies is confirmed only for direct SHM studies with numerical and experimental validation on full-scale bridges, and field validation, and indirect SHM studies with numerical, and experimental validation on full-scale and laboratory-scaled bridges and field validation.

Table 2. Distribution of direct and indirect SHM publications according to journal and conference name.

Journals & conferences	**Number of direct SHM publications**	**Number of indirect SHM publications**
Journal of Civil Structural Health Monitoring	4	-
Applied Sciences	-	4
Structures	2	-
Sensors	2	-
Engineering Failure Analysis	2	-
Railway Engineering Science	-	2
Mechanical Systems and Signal Processing	1	1
Engineering Structures	5	-
Structural Health Monitoring Based on Data Science Techniques	1	-
Reliability Engineering and System Safety	1	-
Journal of Sound and Vibration	-	1
Structure and Infrastructure Engineering	1	-
Journal of Bridge Engineering	1	-
Australian Journal of Structural Engineering	1	-
Buildings	1	-
IEEE Transactions on Industrial Informatics	1	-
Journal of Constructional Steel Research	1	-
Structural Health Monitoring	2	1
Structural Control & Health Monitoring	2	-
Computer-Aided Civil and Infrastructure Engineering	3	-
3rd International Symposium on Life Cycle Civil engineering	1	-
10th European Workshop on Structural Health Monitoring	-	1
6th International Conference on Railway Technology:	-	1
Research, Development and Maintenance		
11th International Conference on Structural Dynamics	-	1
11th European Workshop on Structural Health Monitoring		1

only on direct SHM using vibration-based sensors under the consideration of varying structural states and varying EOCs. In (Vagnoli et al., 2017), 12 studies on damage diagnosis and one study on damage prognosis are referenced. The 12 damage diagnosis-related studies have been published between 2007 and 2016, whereas the one damage prognosis-related study has been published in 2012. In (Wang et al., 2022), four studies on damage diagnosis and one study on damage prognosis are referenced. The four damage diagnosis-related studies have been published between 2019 and 2022, whereas the one damage prognosis-related study has been published in 2021.

The main research gap is the existence of only two review papers on direct SHM, and the absence of review papers on indirect SHM. An additional research gap, based on the state-of-the-art, is that the number of indirect SHM studies is smaller than the number of direct SHM studies. The goal of the current review article is to address the main research gap by reviewing the state-of-the-art on SHM methods applied to steel railway bridges between 2010 and 2025, including both direct and indirect SHM studies. In addition, the review article provides recommendations for future challenges. Also, details on data processing, modeling, SHM methods, the location, type, and geometry of the examined bridges, the location and type of damages, sensing technologies, sensor deployment, and EOCs mentioned in the state-of-the-art are provided. The remaining sections of the article are organized as follows. Sections 2 and 3 present the details about the reviewed studies on direct and indirect SHM, respectively, whereas Section 4 presents recommendations for future challenges. A summary of the study’s conclusions is presented in Section 5.

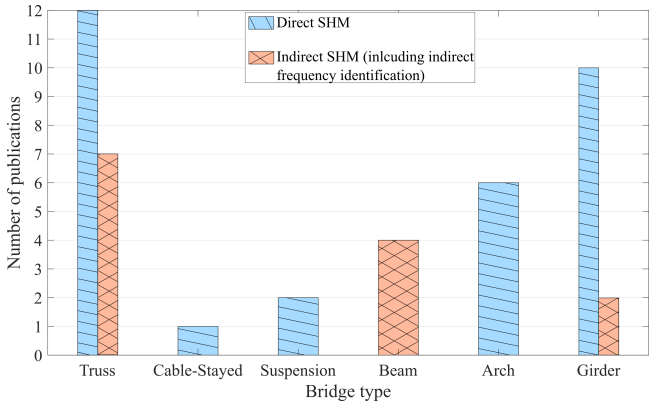

Figure 3. Distribution of direct and indirect SHM publications according to bridge types.

2. DIRECT SHM

Vibration-based direct SHM studies with numerical and experimental validation on full-scale bridges,and field validation are reviewed in this section. In these studies, sensors are installed directly on the bridge and measure structural responses during train passages. The reviewed bridges span a wide range of structural types, lengths, damage types, sensor configurations, and operating environments, all of which shape the design of the monitoring methodology. These characteristics are presented first, followed by the data-processing techniques, modeling approaches, and SHM methods employed for damage diagnosis and prognosis. The section concludes with an assessment of the key strengths and limitations identified across the reviewed studies.

2.1. Overview of Examined Bridges

According to the reviewed direct SHM studies on vibration-based methods for damage diagnosis and prognosis, the methods are applied on bridges located in 14 different countries in Asia (Beskhyroun, Oshima, & Mikami, 2010; Siriwardane, Ohga, Dissanayake, & Kaita, 2010; Beskhyroun, Wegner, & Sparling, 2012; Oshima et al., 2013; Chen, Zhu, Xu, Li, & Cai, 2014; Zhang, Miyamori, & Saito, 2019; Dang, Tatipamula, & Nguyen, 2022; Pourtarki, Ghavifekr, & Afshin, 2023; Li, Ding, Zhao, & Sun, 2022; Lee, Park, Kim, & Kim, 2024), North America (Tochaei, Fang, Taylor, Babanajad, & Ansari, 2021), Australia (Ghiasi, Ng, & Sheikh, 2022; Ghiasi, Moghadda, Ng, Sheikh, & Shi, 2022), and Europe (Leander, Andersson, & Karoumia, 2010; Guo et al., 2012; Neves, Gonzalez, & Karoumi, 2022; Maes, Meerbeeck, Reynders, & Lombaert, 2022; Sarmadi, Entezami, Behkamal, & Michele, 2022; Svendsen, Froseth, Oiseth, & Ronnquist, 2022; Zakharenko et al., 2022; Sangiorgio et al., 2022; Svendsen et al., 2023; Yano, Figueiredo, Silva, Cury, & Moldovan, 2023; Torres, Poveda, Ivorra, & Estevan, 2023; Anastasia, Garcia-Macias, Ubertini, Gattulli, & Ivorra, 2023; Menghini, Leander, & Castiglioni, 2023; Anastasopoulos & Reynders, 2023; Nguyen et al., 2024; Quqa, Palermo, & Marzani, 2024; Armijo & Zamora-Sanchez, 2024; Monti, Rabi, Marella, & Proietti, 2025). Europe and Spain present the highest research activity about direct SHM (Sangiorgio et al., 2022; Torres et al., 2023; Anastasia et al., 2023; Armijo & Zamora-Sanchez, 2024).

Regarding the structural topology of these bridges, the major type is truss (Siriwardane et al., 2010; Guo et al., 2012; Rageh, Linzell, & E., 2018; Svendsen et al., 2022; Dang et al., 2022; Pourtarki et al., 2023; Sangiorgio et al., 2022; Svendsen et al., 2023; Torres et al., 2023; Anastasia et al., 2023; Menghini et al., 2023; Monti et al., 2025). Other types of bridges include girder (Beskhyroun et al., 2010; Oshima et al., 2013; Ghiasi, Ng, & Sheikh, 2022; Leander et al., 2010; Ghiasi, Moghadda, et al., 2022; Beskhyroun et al., 2012; Anastasopoulos & Reynders, 2023; Armijo & Zamora-Sanchez, 2024; Zhang et al., 2019; Lee et al., 2024), arch (Maes et al., 2022; Neves et al., 2022; Sarmadi et al., 2022; Yano et al., 2023; Nguyen et al., 2024; Quqa et al., 2024), cable-stayed (Li et al., 2022), and suspension (Chen et al., 2014; Tochaei et al., 2021). The length of these bridges ranges between 6.45 m (Zhang et al., 2019) and 1290 m (Li et al., 2022). In a few studies, only some spans of the entire bridge are examined (Li et al., 2022; Torres et al., 2023).

The majority of the direct SHM studies investigate field validation (Maes et al., 2022; Neves et al., 2022; Sarmadi et al., 2022; Guo et al., 2012; Ghiasi, Ng, & Sheikh, 2022; Dang et al., 2022; Rageh et al., 2018; Yano et al., 2023; Torres et al., 2023; Pourtarki et al., 2023; Nguyen et al., 2024; Quqa et al., 2024; Li et al., 2022; Ghiasi, Moghadda, et al., 2022; Anastasia et al., 2023; Armijo & Zamora-Sanchez, 2024; Menghini et al., 2023; Monti et al., 2025; Chen et al., 2014; Zakharenko et al., 2022; Leander et al., 2010; Tochaei et al., 2021; Sangiorgio et al., 2022; Siriwardane et al., 2010) and numerical validation on full-scale bridges (Beskhyroun et al., 2010; Maes et al., 2022; Svendsen et al., 2023, 2022; Guo et al., 2012; Ghiasi, Ng, & Sheikh, 2022; Dang et al., 2022; Torres et al., 2023; Pourtarki et al., 2023; Nguyen et al., 2024; Quqa et al., 2024; Ghiasi, Moghadda, et al., 2022; Anastasia et al., 2023; Beskhyroun et al., 2012; Armijo & Zamora-Sanchez, 2024; Menghini et al., 2023; Anastasopoulos & Reynders, 2023; Chen et al., 2014; Sangiorgio et al., 2022; Siriwardane et al., 2010), with fewer studies investigating experimental validation on full-scale bridges (Beskhyroun et al., 2010; Oshima et al., 2013; Svendsen et al., 2023, 2022; Beskhyroun et al., 2012; Anastasopoulos & Reynders, 2023; Zhang et al., 2019; Lee et al., 2024). Additionally, several of the examined railway bridges are decommissioned, and some are replaced by new ones (Beskhyroun et al., 2010; Oshima et al., 2013; Guo et al., 2012; Svendsen et al., 2022, 2023; Beskhyroun et al., 2012; Anastasopoulos & Reynders, 2023; Zhang et al., 2019; Lee et al., 2024).

2.2. Damage Types and Locations

Fatigue is one of the deterioration mechanisms considered in the reviewed studies through its' examination in steel members and connection joints (Tochaei et al., 2021; Sangiorgio et al., 2022; Li et al., 2022; Anastasopoulos & Reynders, 2023; Chen et al., 2014), in relation to cracks with length of 30 cm or even smaller (Tochaei et al., 2021; Anastasopoulos & Reynders, 2023), under retrofitting (Svendsen et al., 2023; Sangiorgio et al., 2022), under corrosion (Svendsen et al., 2022), and during simulations with a 90 % reduction in steel members' cross-section (Chen et al., 2014). Corrosion is another deterioration mechanism considered in the examination of corrosion-induced cracks (Siriwardane et al., 2010), caused by stress application (Menghini et al., 2023), and simulated via a 10 % - 75 % reduction in steel members' cross-section (Ghiasi, Ng, & Sheikh, 2022; Ghiasi, Moghadda, et al., 2022; Quqa et al., 2024).

In some studies, damages not related to a specific deterioration mechanism are examined. Some damages are related to welded/bolted joints, such as removed bolts (Beskhyroun et al., 2010, 2012; Oshima et al., 2013; Svendsen et al., 2022, 2023), stiffness degradation (Dang et al., 2022), reduced strain values by 10 % - 90 % (Rageh et al., 2018), and behavior changes (Monti et al., 2025). Other damages include 10 % - 100 % stiffness reduction (Beskhyroun et al., 2010; Guo et al., 2012; Beskhyroun et al., 2012; Torres et al., 2023), 21 % - 41 % stiffness increase (Maes et al., 2022), 10 % - 40 % elasticity modulus reduction (Pourtarki et al., 2023; Anastasia et al., 2023; Armijo & Zamora-Sanchez, 2024), cracks (Oshima et al., 2013), changed length of influence lines (Zakharenko et al., 2022), pier tilt (Monti et al., 2025), deck degradation (Monti et al., 2025) and 3.21 kg - 1 400 kg attached masses (Zhang et al., 2019; Lee et al., 2024). Also, retrofitting is considered a form of damage that alters the bridge dynamics (Neves et al., 2022; Maes et al., 2022; Sarmadi et al., 2022; Yano et al., 2023). It must be noted that the simulated damages are created via various software applications such as SAP2000 (Beskhyroun et al., 2010; Siriwardane et al., 2010; Beskhyroun et al., 2012; Sangiorgio et al., 2022; Torres et al., 2023; Anastasia et al., 2023), ANSYS (Ghiasi, Ng, & Sheikh, 2022; Ghiasi, Moghadda, et al., 2022; Anastasopoulos & Reynders, 2023; Armijo & Zamora-Sanchez, 2024), Abaqus (Svendsen et al., 2023), MATLAB toolbox Stabil (Maes et al., 2022), MIDAS (Menghini et al., 2023), and Solvia03 (Leander et al., 2010).

In truss bridges, damages are considered at connection joints (Siriwardane et al., 2010; Rageh et al., 2018; Dang et al., 2022; Svendsen et al., 2022, 2023), side, bottom, top, and diagonal members (Guo et al., 2012; Chen et al., 2014; Pourtarki et al., 2023; Li et al., 2022; Sangiorgio et al., 2022; Torres et al., 2023; Anastasia et al., 2023; Menghini et al., 2023; Monti et al., 2025), the mid-span of the deck slab (Monti et al., 2025), and the top of piers (Svendsen et al., 2023). In girder bridges, damages are considered at elements (Oshima et al., 2013), and the bottom and top of girders (Beskhyroun et al., 2010, 2012; Oshima et al., 2013; Zhang et al., 2019; Ghiasi, Ng, & Sheikh, 2022; Ghiasi, Moghadda, et al., 2022; Anastasopoulos & Reynders, 2023; Armijo & Zamora-Sanchez, 2024; Lee et al., 2024). In arch bridges, damages are considered at the arch ribs (Neves et al., 2022; Maes et al., 2022; Sarmadi et al., 2022; Yano et al., 2023; Quqa et al., 2024) and connection joints (Neves et al., 2022; Maes et al., 2022; Sarmadi et al., 2022; Yano et al., 2023). In suspension bridges, damages are examined at connection joints (Tochaei et al., 2021) and bottom, top, and diagonal members (Chen et al., 2014; Tochaei et al., 2021), whereas in cable-stayed bridges, damages are examined at members (Li et al., 2022).

2.3. Sensing Technologies and Deployment

Accelerometers are mostly used for damage diagnosis, including uniaxial (Beskhyroun et al., 2010; Guo et al., 2012; Beskhyroun et al., 2012; Oshima et al., 2013; Zhang et al., 2019; Neves et al., 2022; Maes et al., 2022; Sarmadi et al., 2022; Svendsen et al., 2022; Ghiasi, Ng, & Sheikh, 2022; Ghiasi, Moghadda, et al., 2022; Svendsen et al., 2023; Yano et al., 2023; Torres et al., 2023; Anastasia et al., 2023; Menghini et al., 2023; Lee et al., 2024; Monti et al., 2025), biaxial (Svendsen et al., 2022, 2023; Nguyen et al., 2024), triaxial (Dang et al., 2022; Anastasia et al., 2023; Anastasopoulos & Reynders, 2023), Micro–Electro-Mechanical Systems (MEMS) (Pourtarki et al., 2023; Armijo & Zamora-Sanchez, 2024), and Integrated Electronics Piezo-Electric (IEPE) (Nguyen et al., 2024) accelerometers. The minimum and maximum numbers of accelerometers deployed for monitoring a bridge are one and 56, respectively. These sensors are installed on various bridge parts such as arches (Neves et al., 2022; Maes et al., 2022; Sarmadi et al., 2022; Svendsen et al., 2022, 2023; Yano et al., 2023; Nguyen et al., 2024), sides, bottom, and top of girders (Beskhyroun et al., 2010, 2012; Oshima et al., 2013; Zhang et al., 2019; Ghiasi, Ng, & Sheikh, 2022; Ghiasi, Moghadda, et al., 2022; Anastasopoulos & Reynders, 2023; Nguyen et al., 2024; Armijo & Zamora-Sanchez, 2024; Lee et al., 2024), stringers (Svendsen et al., 2022, 2023), sides, and top of deck (Neves et al., 2022; Maes et al., 2022; Sarmadi et al., 2022; Yano et al., 2023; Torres et al., 2023; Monti et al., 2025), and sides, top, and bottom members (Guo et al., 2012; Pourtarki et al., 2023; Anastasia et al., 2023; Menghini et al., 2023).

Strain gauge sensors are also used for damage diagnosis and prognosis, including strain transducers (Leander et al., 2010; Siriwardane et al., 2010; Chen et al., 2014; Rageh et al., 2018; Neves et al., 2022; Zakharenko et al., 2022; Sangiorgio et al., 2022; Menghini et al., 2023; Quqa et al., 2024; Monti et al., 2025) and optical fiber strain sensors such as Fiber Bragg Grating Sensors (FBGS) (Tochaei et al., 2021; Li et al., 2022; Anastasia et al., 2023; Anastasopoulos & Reynders, 2023).

The minimum and maximum numbers of strain gauge sensors deployed for monitoring a bridge are five and 110, respectively. These sensors are installed on deck (Neves et al., 2022), stringers (Leander et al., 2010; Rageh et al., 2018), arches (Quqa et al., 2024), top, diagonal, bottom and counterweight members (Siriwardane et al., 2010; Chen et al., 2014; Tochaei et al., 2021; Li et al., 2022; Sangiorgio et al., 2022; Anastasia et al., 2023; Menghini et al., 2023; Monti et al., 2025), rails (Leander et al., 2010; Zakharenko et al., 2022) and bottom and top of girders (Leander et al., 2010; Anastasopoulos & Reynders, 2023).

Apart from accelerometers and strain gauge sensors, three to six displacement transducers are installed on girders (Quqa et al., 2024) and joints (Monti et al., 2025). Also, seven inclination sensors are installed on piers (Torres et al., 2023; Monti et al., 2025), deck (Monti et al., 2025), and joints (Menghini et al., 2023), and eight sensors are installed on the tracks for measuring the train weight (Monti et al., 2025). The temperature of air (Sarmadi et al., 2022; Svendsen et al., 2022, 2023) and bridges (Neves et al., 2022; Maes et al., 2022; Yano et al., 2023; Monti et al., 2025) is measured via sensors.

The frequency range over which signals are acquired and analyzed varies. For a low frequency bandwidth, the maximum frequency is up to 50 Hz (Guo et al., 2012; Rageh et al., 2018; Tochaei et al., 2021; Ghiasi, Ng, & Sheikh, 2022; Dang et al., 2022; Pourtarki et al., 2023; Li et al., 2022; Ghiasi, Moghadda, et al., 2022; Anastasia et al., 2023; Quqa et al., 2024; Lee et al., 2024). There are a number of studies where the frequency bandwidth reaches 100 Hz (Anastasopoulos & Reynders, 2023; Monti et al., 2025), 250 Hz (Leander et al., 2010; Svendsen et al., 2022, 2023; Armijo & Zamora-Sanchez, 2024; Monti et al., 2025), 375 Hz (Oshima et al., 2013), 525 Hz (Nguyen et al., 2024), or 825 Hz (Beskhyroun et al., 2010, 2012; Neves et al., 2022; Maes et al., 2022; Sarmadi et al., 2022; Yano et al., 2023). In only one study, the frequency bandwidth is up to 1666 Hz (Zhang et al., 2019).

2.4. Environmental and Operational Conditions

In the reviewed studies, train passages are considered as the main source for the bridge excitation (Leander et al., 2010; Siriwardane et al., 2010; Guo et al., 2012; Chen et al., 2014; Rageh et al., 2018; Neves et al., 2022; Tochaei et al., 2021; Ghiasi, Ng, & Sheikh, 2022; Dang et al., 2022; Pourtarki et al., 2023; Li et al., 2022; Ghiasi, Moghadda, et al., 2022; Zakharenko et al., 2022; Sangiorgio et al., 2022; Yano et al., 2023; Torres et al., 2023; Anastasia et al., 2023; Menghini et al., 2023; Nguyen et al., 2024; Quqa et al., 2024; Armijo & Zamora-Sanchez, 2024; Monti et al., 2025). An electromechanical shaker (Beskhyroun et al., 2010, 2012; Oshima et al., 2013; Zhang et al., 2019; Svendsen et al., 2022, 2023; Anastasopoulos & Reynders, 2023) or an impact hammer (Lee et al., 2024) is also used in a few studies to apply force to the considered bridges, with the bridges being decommissioned. The wind is considered as an excitation source in a number of studies (Maes et al., 2022; Svendsen et al., 2022, 2023; Quqa et al., 2024).

Varying EOCs are considered in fewer than half of the studies on direct SHM. The considered varying operational conditions include train traffic intensity (number of train passages) (Leander et al., 2010; Guo et al., 2012; Rageh et al., 2018; Tochaei et al., 2021; Zakharenko et al., 2022; Li et al., 2022; Quqa et al., 2024), number of train cars (Guo et al., 2012; Zakharenko et al., 2022; Li et al., 2022; Quqa et al., 2024), number of axles (Leander et al., 2010; Zakharenko et al., 2022), axle load (Siriwardane et al., 2010; Rageh et al., 2018; Zakharenko et al., 2022), and train speed (Siriwardane et al., 2010; Guo et al., 2012; Neves et al., 2022; Li et al., 2022; Anastasia et al., 2023; Quqa et al., 2024; Monti et al., 2025). According to these studies, the number of passages of freight and passenger trains varies between two and 520. These trains consist of 1 - 16 cars and travel at a speed of 10 km/h - 50 km/h. The number of axles for the considered cars is up to 40 for passenger trains and 100 for freight trains, with train weight ranging from 9 400 kg to 1 750 000 kg. The most common variation across studies is train speed, while the other operating conditions vary less frequently. Also, trains consisting only of locomotives are considered.

The considered varying environmental conditions include wind speed (Svendsen et al., 2022, 2023), air temperature (Sarmadi et al., 2022; Svendsen et al., 2022, 2023), and bridge temperature (Neves et al., 2022; Maes et al., 2022; Yano et al., 2023; Monti et al., 2025). The wind speed is between 0 km/h and 8 km/h, the air temperature is between 1 ^{o}C and 33 ^{o}C, and the bridge temperature is between -10 ^{o}C and 40 ^{o}C. The air temperature is also simulated by varying steel density by 1

In four studies (Chen et al., 2014; Ghiasi, Ng, & Sheikh, 2022; Ghiasi, Moghadda, et al., 2022; Quqa et al., 2024), synthetic measurement noise is incorporated in the simulated data generated via FEMs of the examined bridges. In studies (Chen et al., 2014; Ghiasi, Ng, & Sheikh, 2022), noise levels between 5 % and 100 % are considered, whereas in studies (Ghiasi, Moghadda, et al., 2022; Quqa et al., 2024), noise levels between 13.97 dB and 45 dB are considered.

2.5. Data processing

Vibration-based methods for direct SHM and damage diagnosis use various types of vibration signals, including acceleration, strain, and displacement. Signal processing techniques are applied to these signals, and they can be grouped into spectral methods, time-frequency representations, and time-domain processing.

Spectral methods are applied for identifying the bridge modal characteristics, including natural frequencies (Maes et al.,

2022; Sarmadi et al., 2022; Ghiasi, Ng, & Sheikh, 2022; Pourtarki et al., 2023; Svendsen et al., 2023; Yano et al., 2023; Torres et al., 2023; Armijo & Zamora-Sanchez, 2024), mode shapes (Beskhyroun et al., 2010; Ghiasi, Ng, & Sheikh, 2022; Pourtarki et al., 2023; Svendsen et al., 2023; Anastasopoulos & Reynders, 2023), mode shape curvatures (Svendsen et al., 2023), Power Spectral Density (PSD) magnitude (Oshima et al., 2013), and Operational Deflection Shapes (ODSs) (Beskhyroun et al., 2012). The spectral methods include Fourier Transformation (FT) spectrum-based Operational Modal Analysis (OMA) (Pourtarki et al., 2023), Fast FT (FFT) spectrum-based OMA (Armijo & Zamora-Sanchez, 2024), PSD-based OMA (Beskhyroun et al., 2010, 2012; Oshima et al., 2013), Covariance-driven Stochastic Subspace Identification (SSI-Cov)-based OMA (Maes et al., 2022; Svendsen et al., 2023; Torres et al., 2023) preceded by Chebyshev type I filtering (Maes et al., 2022) or low-pass filtering (Svendsen et al., 2023), and fast bayesian-based OMA (Ghiasi, Ng, & Sheikh, 2022). There are some studies in which the methods for obtaining natural frequencies (Sarmadi et al., 2022; Yano et al., 2023) and mode shapes (Anastasopoulos & Reynders, 2023) are not clarified.

Time-frequency representations are used for extracting features such as Discrete Wavelet Transform (DWT) coefficients obtained via DWT applied on mode shapes (Beskhyroun et al., 2010), Continuous Wavelet Transformation (CWT) scalograms obtained via CWT (Ghiasi, Ng, & Sheikh, 2022), and Intrinsic Mode Functions (IMFs) obtained via CWT-based Sparse Random Mode Decomposition (SRMD) (Armijo & Zamora-Sanchez, 2024). Additionally, the Empirical Mode Decomposition (EMD) is used for signal denoising preceded by Butterworth filtering (Monti et al., 2025).

Time-domain processing approaches include obtaining Proper Orthogonal Modes (POMs) via Proper Orthogonal Decomposition (POD) (Rageh et al., 2018), Root Mean Square (RMS) (Neves et al., 2022; Nguyen et al., 2024), influence lines and dynamic load factors under multi-band finite impulse response (Li et al., 2022), influence lines (Chen et al., 2014), and vibration energy (Pourtarki et al., 2023). The range of the stress amplitudes and the number of cycles corresponding to these amplitudes are obtained via rainflow counting (Leander et al., 2010; Siriwardane et al., 2010; Sangiorgio et al., 2022; Zakharenko et al., 2022) preceded by Bessel filtering (Leander et al., 2010). In some studies, back-propagation filtering (Neves et al., 2022), and low-pass filtering (Svendsen et al., 2022) followed by resampling are applied to vibration signals. Also, low-pass filtering (Anastasia et al., 2023) or resampling (Anastasopoulos & Reynders, 2023) is applied individually to vibration signals.

2.6. Modeling

Apart from the experimental data used in the reviewed studies on direct SHM, physics-based models, namely Finite Element Models (FEMs), are used in most studies to generate simulated data under various structural states of the examined bridges (Beskhyroun et al., 2010; Leander et al., 2010; Siriwardane et al., 2010; Guo et al., 2012; Beskhyroun et al., 2012; Chen et al., 2014; Maes et al., 2022; Ghiasi, Ng, & Sheikh, 2022; Dang et al., 2022; Pourtarki et al., 2023; Sangiorgio et al., 2022; Svendsen et al., 2023; Torres et al., 2023; Anastasia et al., 2023; Menghini et al., 2023; Anastasopoulos & Reynders, 2023; Nguyen et al., 2024; Quqa et al., 2024; Armijo & Zamora-Sanchez, 2024). The data are used in damage diagnosis and prognosis. In the case of damage diagnosis, the data are used for training data-based models and for developing signal-processing-based and raw-signal-based damage indices.

Data-based models representing the bridge dynamics are partially used for the identification of modal characteristics and damage diagnosis. The models used for modal identification are state-space models identified from raw (Ghiasi, Ng, & Sheikh, 2022; Torres et al., 2023) or processed vibration signals (Maes et al., 2022; Svendsen et al., 2023). The models used for damage diagnosis include feed-forward Neural Networks (NNs) (Rageh et al., 2018; Neves et al., 2022; Nguyen et al., 2024), Convolutional NNs (CNNs) (Zhang et al., 2019; Dang et al., 2022; Ghiasi, Moghadda, et al., 2022), back-propagation NNs (Nguyen et al., 2024), Conditional Generative Adversarial Network (CGAN) models (Lee et al., 2024), linear regression models (Maes et al., 2022; Monti et al., 2025), AutoRegressive (AR) models (Svendsen et al., 2022; Anastasia et al., 2023), Adaptive Neuro-Fuzzy Inference System (ANFIS)-regression models (Nguyen et al., 2024), Radial Basis Function (RBF)-based nonlinear models (Quqa et al., 2024), Gaussian mixture models (GMMs) (Li et al., 2022), and Principal Components Analysis (PCA) models (Guo et al., 2012; Maes et al., 2022; Anastasia et al., 2023).

The data-based models used for damage diagnosis are trained on signal-processing-based features, raw signals, and model-based features. Based on signal-processing-based features obtained in Section 2.5, POMs are used for training feed-forward NNs (Rageh et al., 2018), influence lines and dynamic factors for training GMMs (Li et al., 2022), and IMFs for training CGAN models (Lee et al., 2024). RMS is used for training feed-forward NNs and ANFIS-regression models, natural frequencies for training PCA models (Maes et al., 2022), and filtered vibration signals for training feed-forward NNs (Neves et al., 2022), AR models (Svendsen et al., 2022), and linear regression models (Monti et al., 2025). Raw vibration signals are used for training PCA models (Guo et al., 2012), AR models (Anastasia et al., 2023), and the rest of the data-based models (Zhang et al., 2019; Maes et al., 2022; Dang et

al., 2022; Ghiasi, Moghadda, et al., 2022; Quqa et al., 2024). Model-based features such as the parameters of AR models can be used for training PCA models (Anastasia et al., 2023).

Model-based features such as the parameters of AR models (Svendsen et al., 2022), displacement signals predicted by RBF-based nonlinear models (Quqa et al., 2024), principal components from from PCA models (Guo et al., 2012), and the flexibility provided bylinear regression models (Monti et al., 2025) are used as model-based damage indices. Also, the residual signal of linear regression models (Maes et al., 2022), and PCA models (Maes et al., 2022; Anastasia et al., 2023), the reconstruction error of CGAN models (Lee et al., 2024), and the strain reduction predicted via feed-forward NNs (Rageh et al., 2018) are used as model-based damage indices.

Additionally, signal-processing-based damage indices can be derived from model-based features such as the RMS of feed-forward NNs' reconstruction error (Neves et al., 2022), the RMS of vibration signals predicted via feed-forward NNs (Nguyen et al., 2024), and the RMS of vibration signals predicted via ANFIS-regression models (Nguyen et al., 2024).

Signal-processing-based damage indices and raw-signal-based damage indices can be developed without including any data-based models. Signal-processing-based features (see Section 2.5) can be used as signal-processing-based damage indices, and they include DWT coefficients (Beskhyroun et al., 2010), natural frequencies (Maes et al., 2022; Sarmadi et al., 2022; Ghiasi, Ng, & Sheikh, 2022; Pourtarki et al., 2023; Svendsen et al., 2023; Yano et al., 2023; Torres et al., 2023; Armijo & Zamora-Sanchez, 2024), mode shapes (Ghiasi, Ng, & Sheikh, 2022; Pourtarki et al., 2023; Svendsen et al., 2023; Anastasopoulos & Reynders, 2023), and mode shape curvatures (Svendsen et al., 2023). Other signal-processing-based damage indices include CWT scalograms (Ghiasi, Ng, & Sheikh, 2022), vibration energy (Pourtarki et al., 2023), ODSs (Beskhyroun et al., 2012), PSD magnitude (Oshima et al., 2013), and influence lines (Chen et al., 2014). The raw-signal-based damage indices are developed based on vibration signals in (Guo et al., 2012; Dang et al., 2022; Menghini et al., 2023).

The varying EOCs are treated either implicitly or explicitly. The implicit treatment includes modeling the effects of varying EOCs on dynamics via PCA models (Guo et al., 2012; Maes et al., 2022; Anastasia et al., 2023), nearest-neighbor search (Sarmadi et al., 2022), and filtering techniques (Anastasopoulos & Reynders, 2023). The aim of this treatment is to select features insensitive to changes caused by varying EOCs, assuming they are sensitive to damage (Sarmadi et al., 2022; Anastasopoulos & Reynders, 2023). These features include natural frequencies (Sarmadi et al., 2022), mode shapes (Anastasopoulos & Reynders, 2023), principal components (Guo et al., 2012), and the residual signal of PCA models (Maes et al., 2022; Anastasia et al., 2023). The explicit treatment includes the modeling of the effects of the varying EOCs on the dynamics via natural frequencies (Svendsen et al., 2023), mode shapes (Svendsen et al., 2023), mode shape curvatures (Svendsen et al., 2023), NNs (Neves et al., 2022; Rageh et al., 2018), AR models (Svendsen et al., 2022), linear regression models (Maes et al., 2022; Monti et al., 2025), RBF-based nonlinear models (Quqa et al., 2024), and GMMs (Li et al., 2022). In some models, the continuous, in-operation, measurement of the actual EOCs may be required (Maes et al., 2022). Training the damage diagnosis methods based on both approaches may require vibration data acquired over a wide range of values for the considered EOCs, thus capturing EOC variability. Of course, there are studies that do not consider EOC variability (Beskhyroun et al., 2010, 2012; Oshima et al., 2013; Chen et al., 2014; Ghiasi, Ng, & Sheikh, 2022; Dang et al., 2022; Pourtarki et al., 2023; Ghiasi, Moghadda, et al., 2022; Yano et al., 2023; Torres et al., 2023; Menghini et al., 2023; Nguyen et al., 2024; Armijo & Zamora-Sanchez, 2024; Lee et al., 2024).

2.7. SHM methods

Using the features, models, and damage indices described in Sections 2.5 and 2.6, the reviewed direct SHM studies address two complementary objectives: damage diagnosis, which encompasses detection, localization, and quantification of structural changes, and damage prognosis, which encompasses the estimation of the structural RUL.

2.7.1. Damage Diagnosis

Damage diagnosis methods can either be equipped with data-based models (see Section 2.6) or be model-free. In both methods, damages are diagnosed from changes in damage indices, which are deviations from the baseline.

In the methods equipped with models, the damage indices are model-based damage indices (Guo et al., 2012; Rageh et al., 2018; Maes et al., 2022; Svendsen et al., 2022; Anastasia et al., 2023; Quqa et al., 2024; Lee et al., 2024; Monti et al., 2025) or signal-processing-based damage indices, which are derived from model-based features (Neves et al., 2022; Nguyen et al., 2024) (see the damage indices in Section 2.6). In some studies, the changes in the damage indices are expressed via the Mahalanobis distance (Neves et al., 2022; Li et al., 2022; Yano et al., 2023), Hotelling's T^2 control charts (Anastasia et al., 2023), and the Frechet inception distance (Lee et al., 2024). Based on these indices, damage detection (Rageh et al., 2018; Neves et al., 2022; Maes et al., 2022; Svendsen et al., 2022; Anastasia et al., 2023; Nguyen et al., 2024; Quqa et al., 2024; Lee et al., 2024; Monti et al., 2025), localization (Rageh et al., 2018; Maes et al., 2022; Svendsen et al., 2022; Anastasia et al., 2023), and quantification (Rageh et al., 2018; Monti et al., 2025) are achieved.

In study (Svendsen et al., 2022), the model-based damage indices are combined with machine learning techniques / classifiers, including Support Vector Machine (SVM), K-Nearest Neighbor (KNN), and Random Forest (RF), for the achievement of damage detection, localization, and identification. In study (Guo et al., 2012), the model-based damage indices are combined with K-means clustering for the achievement of damage detection.

In studies (Zhang et al., 2019; Dang et al., 2022; Li et al., 2022; Ghiasi, Moghadda, et al., 2022) where no damage indices are used, the raw-signal-trained NNs and GMMs act as classifiers, and they achieve damage detection (Zhang et al., 2019; Li et al., 2022; Ghiasi, Moghadda, et al., 2022), localization (Zhang et al., 2019; Dang et al., 2022; Ghiasi, Moghadda, et al., 2022), and quantification (Zhang et al., 2019; Dang et al., 2022; Ghiasi, Moghadda, et al., 2022).

In the methods which are model-free, the damage indices are raw-signal-based damage indices (Dang et al., 2022; Menghini et al., 2023) or signal-processing-based damage indices (Beskhyroun et al., 2010, 2012; Oshima et al., 2013; Chen et al., 2014; Sarmadi et al., 2022; Ghiasi, Ng, & Sheikh, 2022; Pourtarki et al., 2023; Svendsen et al., 2023; Yano et al., 2023; Torres et al., 2023; Anastasopoulos & Reynders, 2023; Armijo & Zamora-Sanchez, 2024) (see the damage indices in Section 2.6). In some studies, the changes in the damage indices are expressed via the Modal Assurance Criterion (MAC) and the Coordinate MAC (COMAC) (Beskhyroun et al., 2012). Based on these indices, damage detection (Beskhyroun et al., 2010, 2012; Oshima et al., 2013; Chen et al., 2014; Sarmadi et al., 2022; Dang et al., 2022; Pourtarki et al., 2023; Svendsen et al., 2023; Yano et al., 2023; Torres et al., 2023; Menghini et al., 2023; Anastasopoulos & Reynders, 2023), localization (Beskhyroun et al., 2010, 2012; Oshima et al., 2013; Chen et al., 2014; Ghiasi, Ng, & Sheikh, 2022; Pourtarki et al., 2023; Svendsen et al., 2023; Anastasopoulos & Reynders, 2023), and quantification (Ghiasi, Ng, & Sheikh, 2022) are achieved.

Signal-processing-based damage indices such as natural frequencies (Sarmadi et al., 2022; Ghiasi, Ng, & Sheikh, 2022; Svendsen et al., 2023; Armijo & Zamora-Sanchez, 2024), mode shapes (Svendsen et al., 2023; Ghiasi, Ng, & Sheikh, 2022), mode shape curvatures (Svendsen et al., 2023), and CWT scalograms (Ghiasi, Ng, & Sheikh, 2022) (see Section 2.5) are combined with machine learning techniques/classifiers for the achievement of detection (Sarmadi et al., 2022; Ghiasi, Ng, & Sheikh, 2022; Svendsen et al., 2023; Armijo & Zamora-Sanchez, 2024), localization (Ghiasi, Ng, & Sheikh, 2022; Svendsen et al., 2023; Armijo & Zamora-Sanchez, 2024), identification (Svendsen et al., 2023) and quantification (Ghiasi, Ng, & Sheikh, 2022; Armijo & Zamora-Sanchez, 2024). The machine learning techniques include SVM (Ghiasi, Ng, & Sheikh, 2022; Armijo & Zamora-Sanchez, 2024), KNN (Sarmadi et al., 2022; Ghiasi, Ng, & Sheikh, 2022), K-means clustering (Armijo & Zamora-Sanchez, 2024), and Light Gradient -Boosting Machine (LightGBM) (Armijo & Zamora-Sanchez, 2024). In study (Sarmadi et al., 2022), KNN is combined with the Mahalanobis distance.

Damage detection is achieved by comparing the damage indices with the baseline phase. Damage localization and quantification are treated mainly as classification problems, and they are achieved with the detected damage state being roughly classified either to a prespecified damage state of specific location (Zhang et al., 2019; Svendsen et al., 2022; Ghiasi, Ng, & Sheikh, 2022; Dang et al., 2022; Ghiasi, Moghadda, et al., 2022; Svendsen et al., 2023; Armijo & Zamora-Sanchez, 2024) and magnitude (Zhang et al., 2019; Ghiasi, Ng, & Sheikh, 2022; Dang et al., 2022; Ghiasi, Moghadda, et al., 2022; Armijo & Zamora-Sanchez, 2024) or to the nearest sensor providing the highest value of the damage indicator (Beskhyroun et al., 2010; Oshima et al., 2013; Chen et al., 2014; Rageh et al., 2018; Pourtarki et al., 2023; Anastasia et al., 2023; Anastasopoulos & Reynders, 2023; Monti et al., 2025). NNs (Rageh et al., 2018) and linear regression models (Monti et al., 2025) can treat damage detection and quantification as estimation problems by providing an estimation of either the damage quantity (severity) (Rageh et al., 2018) or a signal-processing-based damage index (flexibility) (Monti et al., 2025), with the estimated magnitudes leading to damage detection.

2.7.2. Damage Prognosis

Damage prognosis in steel bridges is examined under the presence of fatigue, and two types of methods are used for prognosis, the Continuum Damage Mechanics (CDM)-based methods and the Fracture Mechanics (FM)-based methods (Ye et al., 2014). The CDM-based and FM-based methods employ either a deterministic (Leander et al., 2010; Tochaei et al., 2021) or a probabilistic (Tochaei et al., 2021) approach to estimate the RUL.

Based on the deterministic approach in the CDM-based methods, fatigue assessment is based on the consideration of a cumulative increase (linear damage rule) of the fatigue damage under applied cycles. Time-history stress signals corresponding to current, past, and future traffic loads of varying amplitude on the bridges are required for the assessment. The range of stress amplitudes and the number of cycles obtained via rainflow counting applied to the stress signals are used with the S-N (or Wohler or stress-cycles) curves, and the Palmgren-Miner linear damage accumulation rule to obtain the accumulated fatigue damage. The accumulated damage indicates if the fatigue life of the structure has likely been exhausted and failure is imminent (Ye et al., 2014; Leander et al., 2010; Siriwardane et al., 2010; Sangiorgio et al., 2022; Zakharenko et al., 2022).

The simple deterministic approach suffers from the lack of a

consistent definition of failure. Additionally, the Palmgren-Miner rule operates on the assumption that fatigue damage caused by stress cycles is linearly additive, and it doesn't consider the interaction between the different stress cycles, thus leading to inaccurate predictions in some cases (Tochaei et al., 2021).

The FM-based methods under the deterministic approach investigate crack initiation and propagation by considering the stress distribution at the crack tip. These methods employ the Paris-Erdogan fatigue growth law to describe and relate the growth of a crack of a specific size to the stress intensity and the number of fatigue cycles (Ye et al., 2014; Tochaei et al., 2021). The solution of Paris law leads to the number of cycles needed for the propagation of a crack from an initial size to the critical (final) crack length (Ye et al., 2014; Tochaei et al., 2021). As in CDM-based methods, fatigue assessment based on FM-based methods requires time-history stress signals corresponding to current, past, and future traffic loads of varying amplitude (Frøseth & Rönnquist, 2019; Zakharenko et al., 2022). Rainflow counting is applied to the stress signals.

The probabilistic approach of the CDM-based and FM-based methods leads to reliability analysis, which assesses a system's ability to operate properly, and uncertainties are considered via reformulations of the Palmgren-Miner rule and the Paris-Erdogan law (Tochaei et al., 2021). A reliability index, which is a function of the probability of failure, is used as an indicator for structural performance (Tochaei et al., 2021). The reliability index also requires the stress-amplitude range to be obtained via the application of the rainflow counting to stress signals corresponding to current, past, and future traffic loads of varying amplitude (Frøseth & Rönnquist, 2019; Zakharenko et al., 2022).

Estimating RUL requires synthesizing stress signals corresponding to current, past, and future traffic loads of varying amplitudes. To achieve this, experimental stress measurements, a calibrated FEM of the bridge, and a traffic load model are required. Influence lines are extracted from the experimental stress signals through structural identification. In parallel, the FEM of the bridge is calibrated based on the experimental measurements through a model updating process. The traffic load model is defined based on sources such as historical traffic records. This model provides the axle loads, train configurations, speeds, and traffic frequencies needed to represent current, past, and future load scenarios. Stress signals for each traffic scenario are then synthesized by convolving the extracted influence lines with the traffic load model, or, alternatively, by direct simulation, in which the loads are applied to the calibrated FEM. (Siriwardane et al., 2010; Froseth, Ronnquist, Cantero, & Oiseth, 2017; Frøseth & Rönnquist, 2019; Zakharenko et al., 2022).

2.8. Strengths and limitations

The main characteristic of direct SHM is the installation of sensors and data acquisition systems on bridges. This installation provides remote, continuous monitoring with a constant stream of vibration and environmental data (Rageh et al., 2018; Neves et al., 2022; Maes et al., 2022; Sarmadi et al., 2022; Sangiorgio et al., 2022; Svendsen et al., 2023; Yano et al., 2023; Torres et al., 2023; Quqa et al., 2024; Monti et al., 2025). Additionally, a distributed network of bridge-based sensors can cover the entire structure and capture both global and local responses (Svendsen et al., 2023). These responses are captured at the source, meaning direct SHM is sensitive to local changes in stiffness, damping, or mass distribution caused by damage (Corbally & Malekjafarian, 2023). Moreover, bridge-based sensors yield high-quality structural dynamic features, such as natural frequencies, mode shapes, influence lines, and strain, which are well-established damage-sensitive indicators (Chen et al., 2014; Maes et al., 2022; Pourtarki et al., 2023; Yano et al., 2023; Anastasopoulos & Reynders, 2023). Another advantage of direct SHM is that it allows sensors to be placed at multiple locations (deck and truss elements) across the bridge, thus providing spatially distributed information that enables damage localization (Oshima et al., 2013; Chen et al., 2014; Rageh et al., 2018; Wang et al., 2022; Anastasia et al., 2023; Monti et al., 2025). Direct SHM has been extensively validated on real railway bridges worldwide across a wide range of bridge types and lengths (see Section 2.1).

Direct SHM has a developed and validated framework for damage detection, localization, quantification, and prognosis. The reviewed studies show that between 12 and 32 sensors can be used for damage detection in bridges with lengths of 91.8 m – 1290 m (Neves et al., 2022; Li et al., 2022; Yano et al., 2023; Monti et al., 2025). Small defects such as loose bolts (Svendsen et al., 2022, 2023), and fatigue cracks (Anastasopoulos & Reynders, 2023), as well as damage-induced changes in structural response, including more than 20 % reduction in measured strain (Rageh et al., 2018), can be detected under varying EOCs. Also, damage localization and quantification under varying EOCs can be achieved successfully (Rageh et al., 2018; Svendsen et al., 2022, 2023; Monti et al., 2025). The diagnosis results in steel bridges are successful, and they include 20 % false positive and 80 % true positive rates based on Receiver Operating Characteristic (ROC) curves in (Neves et al., 2022), 4.3 % misclassified cases in (Svendsen et al., 2022), 5.4 % misclassified cases in (Yano et al., 2023), 0.001 % misclassified cases in (Armijo & Zamora-Sanchez, 2024), and 0.64 % misclassified cases in (Zhang et al., 2019). Additionally, the application of the prognosis methods examined in most studies has yielded successful RUL estimates (Siriwardane et al., 2010; Tochaei et al., 2021; Zakharenko et al., 2022; Sangiorgio et al., 2022).

The main disadvantage of direct SHM is that the mass de-

ployment of direct SHM systems and the maintenance of instrumentation on the large number of unmonitored bridges entail high, prohibitive costs (Bernardini et al., 2021, 2025b). As a result, only spans rather than the entire bridge are monitored in some studies (Li et al., 2022; Torres et al., 2023). Additionally, the direct SHM methods lack portability and hinder continuous monitoring, as sensor lifespans are generally shorter than those of bridges. Lightweight sensors are susceptible to damage in harsh environments with high pressure or vibration (Malekjafarian, McGetrick, & OBrien, 2015). Increasing the precision of damage localization and quantification, which are treated as classification problems, requires more sensors or prespecified damage types, leading to a larger baseline phase for the damage diagnosis methods. Also, the training and validation of damage diagnosis methods based on data from bridge damage states are mostly performed using simulated data. The simulated data are generated via an FEM of the examined bridge, with the FEM's uncertainty, fidelity, boundary-condition assumptions, and material-property assumptions (train–bridge interaction, track irregularities, torsion/warping, braking dynamics, linearity, etc) affecting the damage diagnosis success (Dang et al., 2022; Svendsen et al., 2023). The simulated damage scenarios may not reflect real damage behavior.

There are a few damage diagnosis methods that have difficulties in detecting small damages of less than 20 % reduction in measured strain (Rageh et al., 2018), and less than 40 % reduction in the elasticity modulus (Anastasia et al., 2023). Additionally, they suffer from multiple false alarms (Anastasia et al., 2023), exhibit 64 % misclassifications based on natural frequencies and 24 % misclassifications based on deflection (Torres et al., 2023), and have difficulty localizing multiple damages (Beskhyroun et al., 2010, 2012). No decision threshold is used for damage diagnosis in most of the studies (Beskhyroun et al., 2010, 2012; Oshima et al., 2013; Chen et al., 2014; Zhang et al., 2019; Neves et al., 2022; Li et al., 2022; Ghiasi, Moghadda, et al., 2022; Menghini et al., 2023; Anastasopoulos & Reynders, 2023; Nguyen et al., 2024; Quqa et al., 2024; Armijo & Zamora-Sanchez, 2024). Additionally, the effectiveness of damage detectability and localization depends on the sensors' locations and numbers, and the methods' performance degrades with reduced sensor networks (Beskhyroun et al., 2010, 2012; Oshima et al., 2013; Chen et al., 2014; Rageh et al., 2018; Zhang et al., 2019; Li et al., 2022; Svendsen et al., 2022, 2023; Anastasia et al., 2023; Quqa et al., 2024; Monti et al., 2025).

Some methods' effectiveness in damage diagnosis is examined based only on data from retrofitting (Neves et al., 2022; Maes et al., 2022; Sarmadi et al., 2022; Yano et al., 2023) and from the healthy state (Rageh et al., 2018; Li et al., 2022). Additionally, some methods are validated based only on simulated data generated under damage states (Guo et al., 2012; Chen et al., 2014; Ghiasi, Ng, & Sheikh, 2022; Dang et al., 2022; Pourtarki et al., 2023; Ghiasi, Moghadda, et al., 2022; Torres et al., 2023; Anastasia et al., 2023; Menghini et al., 2023; Nguyen et al., 2024; Quqa et al., 2024; Armijo & Zamora-Sanchez, 2024) and a few damage cases (Beskhyroun et al., 2010, 2012; Oshima et al., 2013; Chen et al., 2014; Zhang et al., 2019; Sarmadi et al., 2022; Pourtarki et al., 2023).

In some of the damage diagnosis methods, it is not clear if the effectiveness is tested only with damage cases considered in the training phase (Guo et al., 2012; Zhang et al., 2019; Sarmadi et al., 2022; Svendsen et al., 2022; Monti et al., 2025), whereas in other methods, the effectiveness is examined based only on damage scenarios, with no results on the methods' false alarm rate (Beskhyroun et al., 2010, 2012; Oshima et al., 2013; Rageh et al., 2018; Neves et al., 2022; Maes et al., 2022; Dang et al., 2022; Ghiasi, Moghadda, et al., 2022; Yano et al., 2023; Torres et al., 2023; Quqa et al., 2024; Armijo & Zamora-Sanchez, 2024). Finally, the variability of EOCs (temperature, train-speed, axle-load) masks the damage-related changes (Maes et al., 2022), influences measured responses (Zhang et al., 2019), and creates difficulty in separating the EOC effects from damage effects (Maes et al., 2022). The effects of changes in EOCs are not considered in many of the reviewed studies (Beskhyroun et al., 2010, 2012; Chen et al., 2014; Rageh et al., 2018; Zhang et al., 2019; Neves et al., 2022; Ghiasi, Ng, & Sheikh, 2022; Dang et al., 2022; Pourtarki et al., 2023; Svendsen et al., 2023; Yano et al., 2023; Torres et al., 2023; Menghini et al., 2023; Armijo & Zamora-Sanchez, 2024).

The application of CDM-based and FM-based damage prognosis methods shows that RUL is estimated based on structural component failure rather than system-level failure (Tochaei et al., 2021). Additionally, applying some damage prognosis methods based on the accumulation rule may indicate that failure is imminent, even though no cracks have been detected (Leander et al., 2010). This error occurs because CDM-based and FM-based methods, based on the deterministic approach, do not account for uncertainties such as material and load uncertainties, and thus do not provide a realistic estimate of the RUL for steel bridges (Tochaei et al., 2021).

Table 3 presents a summary of the main information about the direct SHM studies.

3. INDIRECT FREQUENCY IDENTIFICATION AND SHM

This section reviews the indirect SHM studies with numerical validation on full-scale bridges, experimental validation on laboratory-scaled bridges, and field validation. In these studies, structural responses are measured by sensors installed on passing trains rather than on the bridges themselves. The reviewed studies span frequency identification, which recovers bridge natural frequencies from train-borne measurements as an enabling monitoring task, and damage diagnosis, which targets damage detection and localization through signal-processing

Table 3. Review of studies about direct SHM in railway bridges.

Reference	**Bridge type**	**Damage type**	**Sensor type**	**Validation type**	**Environmental variable**	**Operational variable**	**Data processing**	**Modeling**	**SHM method**	**Objective**
(Beskhyroun et al., 2010)	Girder	Removed bolts, stiffness reduction	Accelerometers	Experimental, numerical	-	-	PSD-based OMA, DWT	-	Changes in DWT coefficients	Damage detection, localization
(Maes et al., 2022)	Arch	Stiffness increase	Accelerometers, bridge temperature sensors	Field, numerical	Bridge temperature	-	Chebyshev type I filtering, SSI-Cov-based OMA	State space models, linear regression models, PCA models	Changes in residual signal of the linear regression & PCA models	Damage detection, localization
(Neves et al., 2022)	Arch	Retrofitting	Accelerometers, strain gauges, bridge temperature sensors	Field	Bridge temperature	Train speed	Back-propagation filtering, resampling	Feed-forward NNs	Changes in RMS of the NNs' reconstruction error expressed via the Mahalanobis distance	Damage detection
(Oshima et al., 2013)	Girder	Removed bolts, cracks	Accelerometers	Experimental	-	-	PSD-based OMA	-	Changes in PSD magnitude	Damage detection, localization
(Sarmadi et al., 2022)	Arch	Retrofitting	Accelerometers, air temperature sensors	Field	Air temperature	-	-	-	Changes in natural frequencies expressed via KNN & the Mahalanobis distance	Damage detection
(Svendsen et al., 2023)	Truss	Fatigue under retrofitting, removed bolts	Accelerometers, air temperature sensors	Experimental, numerical	Wind speed, air temperature	-	Low-pass filtering, SSI-Cov-based OMA	State space models	Changes in natural frequencies & mode shapes & mode shape curvatures	Damage detection, localization, identification

Table 3. Cont.

Reference	Bridge type	Damage type	Sensor type	Validation type	Environmental variable	Operational variable	Data processing	Modeling	SHM method	Objective
(Svendsen et al., 2022)	Truss	Corrosion, removed bolts	Accelerometers, air temperature sensors	Experimental, numerical	Wind speed, air temperature	-	Low-pass filtering, resampling	AR models	Changes in AR parameters expressed via SVM, KNN, RF	Damage detection, localization, identification
(Guo et al., 2012)	Truss	Stiffness reduction	Accelerometers	Field, numerical	-	Number of train passages & train cars, train speed	-	PCA models	Changes in principal components of PCA models	Damage detection
(Ghiasi, Ng, & Sheikh, 2022)	Girder	Corrosion simulated by cross-section reduction	Accelerometers	Field, numerical	-	-	Fast bayesian-based OMA, CWT	State-space models	Changes in natural frequencies & mode shapes & CWT scalograms expressed via SVM, KNN	Damage detection, localization, quantification
(Dang et al., 2022)	Truss	Stiffness degradation	Accelerometers	Field, numerical	-	-	-	CNNs	CNNs acting as classifier	Damage detection, localization, quantification
(Rageh et al., 2018)	Truss	Reduced strain	Strain gauges	Field	-	Number of train passages, axle load	POD	Feed-forward NNs	Strain reduction predicted via the NNs	Damage detection, localization, quantification

Table 3. Cont.

Reference	Bridge type	Damage type	Sensor type	Validation type	Environmental variable	Operational variable	Data processing	Modeling	SHM method	Objective
(Yano et al., 2023)	Arch	Retrofitting	Accelerometers, bridge temperature sensors	Field	Bridge temperature	-	-	-	Changes in natural frequencies expressed via the Mahalanobis distance	Damage detection
(Torres et al., 2023)	Truss	Stiffness reduction	Accelerometers, inclination sensors	Field, numerical	-	-	SSI-Cov-based OMA	State-space models	Changes in natural frequencies	Damage detection
(Pourtarki et al., 2023)	Truss	Elasticity modulus reduction	Accelerometers	Field, numerical	-	-	FT-spectrum-based OMA	-	Changes in natural frequencies & mode shapes & vibration energy	Damage detection, localization
(Nguyen et al., 2024)	Arch	-	Accelerometers	Field, numerical	-	-	-	Back-propagation NNs, feed-forward NNs, ANFIS-regression models	Changes in the RMS of the vibration signals predicted via the NNs and regression models	Damage detection
(Quqa et al., 2024)	Arch	Corrosion simulated by cross-section reduction	Strain gauges, displacement transducers	Field, numerical	-	Number of train passages & train cars, train speed	-	RBF-based nonlinear models	Changes in the predicted displacement signals predicted via RBF-based nonlinear models	Damage detection

Table 3. Cont.

Reference	Bridge type	Damage type	Sensor type	Validation type	Environmental variable	Operational variable	Data processing	Modeling	SHM method	Objective
(Li et al., 2022)	Cable-stayed	Fatigue	Strain gauges	Field	-	Number of train passages & train cars, train speed	-	GMMs	GMMs acting as classifier and combined with the Mahalanobis distance	Damage detection
(Ghiasi, Moghadda, et al., 2022)	Girder	Corrosion simulated by cross-section reduction	Accelerometers, displacement transducers	Field, numerical	-	-	-	CNNs	CNNs acting as classifier	Damage detection, localization, quantification
(Anastasia et al., 2023)	Truss	Elasticity modulus reduction	Accelerometers, strain gauges	Field, numerical	-	Train speed	Low-pass filtering	AR models, PCA models	Changes in the PCA models' residual signal expressed via the Hotelling's T^2 control charts	Damage detection, localization
(Beskhyroun et al., 2012)	Girder	Removed bolts, stiffness reduction	Accelerometers	Experimental, numerical	-	-	PSD-based OMA	-	Changes in ODSs expressed via MAC & COMAC	Damage detection, localization
(Armijo & Zamora-Sanchez, 2024)	Girder	Elasticity modulus reduction	Accelerometers	Field, numerical	-	-	FFT spectrum-based OMA, SRMD	-	Changes in natural frequencies expressed via SVM, K-means clustering, LightGBM	Damage detection, localization, quantification

Table 3. Cont.

Reference	Bridge type	Damage type	Sensor type	Validation type	Environmental variable	Operational variable	Data processing	Modeling	SHM method	Objective
(Menghini et al., 2023)	Truss	Corrosion due to stress application	Accelerometers, strain gauges, inclination sensors	Field, numerical	-	-	-	-	Changes in vibration (stress) signals	Damage detection
(Anastasopoulos & Reynders, 2023)	Girder	Fatigue related to cracks	Accelerometers, strain gauges	Experimental, numerical	-	-	Resampling	-	Changes in mode shapes	Damage detection, localization
(Monti et al., 2025)	Truss	Behavior changes, pier tilt, deck degradation	Strain gauges, inclination sensors, weight sensors, bridge temperature sensors	Field	Bridge temperature	Train speed	Butterworth filtering, EMD	Linear regression models	Changes in flexibility obtained via linear regression models	Damage detection, quantification
(Chen et al., 2014)	Suspension	Fatigue examined via cross-section reduction	Strain gauges	Field, numerical	-	-	-	-	Changes in influence lines	Damage detection, localization
(Zhang et al., 2019)	Girder	Attached masses	Accelerometers	Experimental	-	-	-	CNNs	CNNs acting as classifier	Damage detection, localization, quantification

Table 3. Cont.

Reference	Bridge type	Damage type	Sensor type	Validation type	Environmental variable	Operational variable	Data processing	Modeling	SHM method	Objective
(Lee et al., 2024)	Girder	Attached masses	Accelerometers	Experimental	-	-	-	CGAN models	Changes in reconstruction error of CGAN models expressed via the Frechet inception distance	Damage detection
(Zakharenko et al., 2022)	-	Changed length of influence lines	Strain gauges	Field	-	Number of train passages & train cars & axles, axle load	Rainflow counting	-	S-N curves, Palmgren-Miner rule	Damage prognosis
(Leander et al., 2010)	Girder	Fatigue risk	Strain gauges	Field	-	Number of train passages & axles	Bessel filtering, rainflow counting	-	S-N curves, Palmgren-Miner rule	Damage prognosis
(Tochaei et al., 2021)	Suspension	Cracks	Strain gauges	Field	-	Number of train passages	-	-	S-N curves, Paris law	Damage prognosis
(Sangiorgio et al., 2022)	Truss	Fatigue under retrofitting	Strain gauges	Field, numerical	-	-	Rainflow counting	-	S-N curves, Palmgren-Miner rule	Damage prognosis
(Siriwardane et al., 2010)	Truss	Cracks due to corrosion	Strain gauges	Field, numerical	-	Axle load, train speed	Rainflow counting	-	S-N curves, Palmgren-Miner rule	Damage prognosis

and data-driven frameworks. Frequency identification supports the SHM workflow. In indirect SHM, the data processing pipeline depends not only on bridge and damage characteristics but also on vehicle dynamics, sensor placement on the train, and the interaction between train, track, and bridge. These contextual factors are presented first, followed by the data processing, modeling, and SHM methods. The section concludes with an assessment of strengths and limitations.

3.1. Overview of Examined Bridges

Many existing studies on railway bridges using indirect sensing focus on steel bridges located in Europe, with a strong concentration in Italy (Carnevale, Collina, & Peirlinck, 2019; Bernardini, Carnevale, Somaschini, Matsuoka, & Collina, 2020; Bernardini, Bono, & Collina, 2025a; Bernardini et al., 2025b), alongside case studies from Austria (Reiterer, Bettinelli, Stollwitzer, Schellander, & Fink, 2022; Reiterer, Bettinelli, Schellander, Stollwitzer, & Fink, 2023), Portugal (Braganca, Souza, & Bittencourt, 2024), Germany (Rupp et al., 2023; Lorenzen, Rupp, & Hubler, 2024), and Switzerland (Stour, Gres, Dertimanis, Ancu, & Chatzi, 2025). This geographical distribution reflects the substantial research activity in Europe on indirect railway bridge monitoring, particularly under train-induced dynamic excitation.

In terms of structural typology, the predominant type of the examined bridges is truss, with a notable prevalence of Warren-type trusses and general truss configurations (Bernardini et al., 2020; Bernardini et al., 2021; Braganca et al., 2024; Bernardini, Matsuoka, & Collina, 2024; Bernardini et al., 2025a, 2025b; Stour et al., 2025). Several studies also investigate beam or girder bridges (Carnevale et al., 2019; Reiterer et al., 2022; Hajializa deh, 2023; Rupp et al., 2023; Reiterer et al., 2023; Lorenzen et al., 2024). Reported bridge spans range from short spans of approximately 13.2 m (Carnevale et al., 2019) to medium spans of about 33.3 m (girder bridge) (Reiterer et al., 2022, 2023). Multiple truss bridges fall within the 21 m range (Bernardini et al., 2020; Braganca et al., 2024), while some extend to longer spans of approximately 60 m - 65 m (Bernardini et al., 2024; Stour et al., 2025). Overall, the reviewed span range covers short- to medium-span railway bridges (approximately 13 m to 65 m), providing a meaningful basis for performance comparisons across different structural typologies and span lengths. None of the reviewed studies investigates decommissioned bridges.

Several studies focus exclusively on frequency identification (Reiterer et al., 2022, 2023; Rupp et al., 2023; Bernardini et al., 2024; Stour et al., 2025; Lorenzen et al., 2024), where field-based investigations constitute the primary contribution. This emphasis demonstrates that frequency identification research is strongly oriented toward practical deployment and real measurement conditions rather than purely numerical benchmarking. However, when the scope shifts toward broader SHM objectives, most analyses rely on validated numerical models representing full-scale bridges (Carnevale et al., 2019; Bernardini et al., 2020; Bernardini et al., 2021; Reiterer et al., 2022; Braganca et al., 2024; Bernardini et al., 2025a, 2025b). Only a limited number of studies investigate field validation (Bernardini et al., 2025a) and experimental validation on laboratory-scale train–bridge interaction systems (Hajializa deh, 2023).

3.2. Damage Types and Locations

The reviewed studies primarily consider stiffness-related damage mechanisms, which represent structural degradation. These include loose bolts or cracked welds at connections, modeled through reductions in elasticity modulus (Bernardini et al., 2021) and stiffness (Bernardini et al., 2020; Carnevale et al., 2019; Braganca et al., 2024). Stiffness reductions of 10 % (Bernardini et al., 2025b) to 70 % (Carnevale et al., 2019) are used to simulate progressive deterioration. Some studies also consider corrosion-induced deterioration by simultaneously reducing the material density and the elasticity modulus to represent material loss, along with reductions in flexural and axial stiffness (Bernardini et al., 2025a, 2025b). In (Hajializa deh, 2023), damages are simulated by 5.5 kg - 10 kg attached masses. The simulated damage scenarios are generated using ADTreS (Bernardini et al., 2025a) and the VSI tool, which integrates ANSYS and MATLAB (Bernardini et al., 2020; Braganca et al., 2024).

Damage locations vary depending on bridge type. For truss bridges, damage is typically introduced in specific members such as diagonals and lower chord members (Braganca et al., 2024), cross-girders (Bernardini et al., 2025a, 2025b), and connection joints (Bernardini et al., 2020; Bernardini et al., 2021). For beam and girder bridges, stiffness reductions are commonly applied at mid-span (Carnevale et al., 2019) or near critical load-carrying regions such as supports (Hajializa deh, 2023).

3.3. Sensing Technologies and Deployment

Accelerometers are the dominant sensing technology, enabling condition assessment without the need for permanent bridge instrumentation. These sensors are installed on moving trains, including bogies, wheelsets, car bodies, and bogie frames. Study (Bernardini et al., 2024) reports train-based sensing using two accelerometers mounted on the bogie. Study (Reiterer et al., 2022) reports 27 acceleration measurement points on the train, with uniaxial acceleration responses numerically obtained from a computational model. In several studies, a hybrid sensing approach is adopted, where additional sensors are installed directly on the bridge, primarily on the main girders (Rupp et al., 2023; Reiterer et al., 2023; Lorenzen et al., 2024). Notably, study (Lorenzen et al., 2024) reports a large-scale configuration with 44 uniaxial accelerometers on

the bridge and eight on the train. Study (Stour et al., 2025) deploys seven triaxial accelerometers at both bridge and train-related locations, including outer bridge positions and axle boxes, capturing multi-directional vibration content.

Speed sensors and train-mounted velocimeters are occasionally used to measure train velocity (Bernardini et al., 2021; Rupp et al., 2023; Bernardini et al., 2025b). Strain gauges installed on bridge girders are also reported in (Rupp et al., 2023). Environmental sensors such as thermocouples are rarely used (Rupp et al., 2023), and displacement sensors are generally limited to controlled simulations or validation scenarios.

Frequency ranges analyzed vary across studies. Some studies focus on the low-frequency bandwidth, with a maximum frequency of approximately 15 Hz (Reiterer et al., 2022; Bernardini et al., 2024), consistent with serviceability-governing global bridge modes. Other studies extend the bandwidth up to 70 Hz (Carnevale et al., 2019) to capture localized dynamics and higher-mode responses. Reported frequency bandwidths vary significantly, ranging from 1 200 Hz (Reiterer et al., 2023) to 12 000 Hz (Stour et al., 2025), enabling broadband dynamic analysis. Despite these variations, the emphasis across most studies remains on low-frequency characteristics relevant to stiffness-related damage detection.

3.4. Environmental and Operational Conditions

Train passages and track irregularities serve as the primary excitation source, either modeled numerically via vehicle–bridge interaction frameworks (Carnevale et al., 2019; Bernardini et al., 2020; Reiterer et al., 2022; Braganca et al., 2024; Bernardini et al., 2025a) or observed in field deployments (Rupp et al., 2023; Reiterer et al., 2023; Bernardini et al., 2024; Lorenzen et al., 2024; Stour et al., 2025).

Operational variability plays a central role in the reviewed literature. Key operational conditions include train speed, number of cars, axle configuration, axle loads, and traffic frequency. In study (Bernardini et al., 2025b), passenger train traffic intensity varies between 5 and 40 passages. Each train consists of five cars (two axles per car), with axle loads ranging from 110 kN to 170 kN. Speeds of 80 km/h and 130 km/h are examined. Study (Reiterer et al., 2022) considers 11-car passenger trains with speeds between 135 km/h and 165 km/h. In study (Carnevale et al., 2019), heavy-haul and lightweight trains are modeled with four to five carbodies (12–16 axles) and axle loads of approximately 15 725 kg - 16 142 kg per axle, operating between 80 km/h and 140 km/h. Study (Bernardini et al., 2025a) analyses 40 passenger trains (eight cars, 32 axles) with axle loads derived from weigh-in-motion data of 268 passages and speeds between 80 km/h and 130 km/h. In experimental study (Hajializa deh, 2023), scaled train–bridge systems with prescribed masses operating at low speeds (3.2 km/h - 9.6 km/h) are used. Freight-dominated studies examine five-wagon trains with variable wagon masses (total mass of 27 000 kg to 47 173 kg) and speeds ranging from 40 km/h to 100 km/h (Bernardini et al., 2020; Braganca et al., 2024).

Several frequency-identification studies examine wide speed envelopes. For instance, study (Reiterer et al., 2023) considers operational speeds of 135 km/h - 165 km/h and simulation speeds up to 420 km/h. Study (Rupp et al., 2023) examines speeds from 10 km/h to 200 km/h with a compact four-car configuration. Study (Bernardini et al., 2024) investigates three speed cases (107 km/h, 123 km/h, 188 km/h) and uniquely quantifies track irregularity (standard deviation 1.9 mm; peak-to-peak 9 mm), highlighting its influence on indirect frequency identification. Overall, train speed variation is consistently incorporated across studies, whereas axle load variation and traffic intensity are less frequently considered.

Environmental variability receives comparatively limited attention. Field studies are conducted under ambient outdoor conditions subject to wind and temperature variations (Reiterer et al., 2022; Rupp et al., 2023; Reiterer et al., 2023; Lorenzen et al., 2024; Stour et al., 2025), yet explicit mitigation strategies are rarely implemented. Some numerical studies indirectly account for temperature effects by varying material stiffness (Braganca et al., 2024). However, comprehensive environmental modeling remains limited.

Finally, several numerical investigations incorporate synthetic measurement noise. Studies (Bernardini et al., 2020; Bernardini et al., 2021) consider noise levels up to 10 %, while study (Braganca et al., 2024) assumes 5 % noise level, enabling robustness assessment of SHM frameworks under more realistic measurement disturbances.

3.5. Data processing

The indirect SHM studies rely on train-borne acceleration signals measured at bogies, wheelsets, or car bodies. The data processing techniques applied to these signals can be grouped into spectral methods for frequency identification, time-frequency representations for damage diagnosis, and time-domain processing.

Spectral methods are the most common processing approach and are predominantly used for the identification of natural frequencies. These methods include FFT spectrum-based OMA preceded by low-pass filtering (Reiterer et al., 2022, 2023), Stochastic Subspace Identification (SSI)-based OMA applied to the post-crossing decay segment, and preceded by Butterworth low-pass filtering combined with maximum oscillation-width extraction (Rupp et al., 2023). Additionally, the spectral methods include indirect resonance curve maxima (Rupp et al., 2023), FFT-spectrum-based OMA applied to low-pass-filtered time-shifted subtraction of onboard accelerations from multiple bogies for track-irregularity suppression (Bernardini et al., 2024), and Frequency Domain Decomposition (FDD)-based OMA (Stour et al., 2025). Also, they include SSI-Cov-based

OMA, Auto-Regressive Moving Average with eXogenous input (ARMAX) model-based OMA preceded by the estimation of contact forces via a Dual Kalman Filter (DKF) framework (Stour et al., 2025), and FFT-based OMA applied on residual responses formed by adjacent-vehicle subtraction with time shift (Lorenzen et al., 2024).

Time-frequency representations are used as front-end feature extractors for damage diagnosis rather than for direct frequency identification. These include CWT with complex Morlet wavelets (Bernardini et al., 2021, 2025a, 2025b), Short-Time Fourier Transform (STFT) (Hajializa deh, 2023), Wavelet Scattering Transform (WST) preceded by Chebyshev II low-pass filtering (Braganca et al., 2024), and combined EMD and Hilbert transform into Hilbert-Huang Transform (HHT) (Bernardini et al., 2021). The resulting features include CWT coefficient maps and averaged wavelet-coefficient curves (Bernardini et al., 2021, 2025a, 2025b), STFT spectrogram images (Hajializa deh, 2023), multiscale WST coefficients (Braganca et al., 2024), and HHT instantaneous energy profiles (Bernardini et al., 2021).

Time-domain processing approaches avoid explicit spectral or modal identification. These include quasi-static component isolation via low-pass filtering combined with moving-window RMS computation (Carnevale et al., 2019), and roll-acceleration differencing formed as the right-minus-left difference of wagon-side accelerations after low-pass Butterworth filtering over the 0 Hz - 50 Hz band (Bernardini et al., 2020). The resulting features include position-dependent RMS profiles (Carnevale et al., 2019) and roll-acceleration signals encoding structural asymmetry (Bernardini et al., 2020).

3.6. Modeling

Physics-based vehicle-bridge interaction models are employed in most of the reviewed studies and serve three distinct roles: as the core simulation environment in which signal-processing-based damage indices are developed and evaluated (Carnevale et al., 2019; Bernardini et al., 2020; Bernardini et al., 2021); as the data generation engine for training data-based models (Hajializa deh, 2023; Braganca et al., 2024; Bernardini et al., 2025a, 2025b); and as validation or benchmarking tools for frequency identification, either by verifying field-observed spectral peaks against numerically predicted modes (Reiterer et al., 2022, 2023; Bernardini et al., 2024) or by embedding the physics-based formulation within the identification method itself (Lorenzen et al., 2024; Stour et al., 2025). Only studies (Rupp et al., 2023) and (Hajializa deh, 2023) operate without a physics-based model, relying entirely on field measurements and scaled-bridge experiments, respectively.

Data-based models are used for damage diagnosis and frequency identification. The models used for frequency identification include state-space models (Rupp et al., 2023; Stour et al., 2025) and ARMAX models (Stour et al., 2025), both identified from processed vibration signals. For the ARMAX models, the model parameters are estimated from DKF-reconstructed contact forces, yielding natural frequency estimates as the monitoring output (Stour et al., 2025). The models used for damage diagnosis include sparse autoencoder NNs (AENNs) (Braganca et al., 2024; Bernardini et al., 2025a, 2025b), CNNs (Hajializa deh, 2023), and PCA models (Braganca et al., 2024).

The data-based models are trained on signal-processing-based features obtained in Section 3.5, and produce model-based damage indices or monitoring outputs. AENNs are trained on averaged CWT coefficient curves resampled to fixed spatial grids (Bernardini et al., 2025a, 2025b) or on multiscale WST coefficients (Braganca et al., 2024), both extracted from baseline undamaged responses. CNNs are trained on STFT spectrogram images (Hajializa deh, 2023). Model-based features, such as the absolute reconstruction error of AENNs, can be used to train PCA models (Braganca et al., 2024). Model-based features derived from AENNs and PCA models can be used as model-based damage indices. These features include the batch mean absolute reconstruction error from AENNs (Bernardini et al., 2025a, 2025b), and the residual signal of PCA models (Braganca et al., 2024).

Signal-processing-based monitoring outputs and signal-processing-based damage indices can also be developed without data-based models. For frequency identification, spectrum magnitude (peaks) and resonance-curve maxima serve as monitoring outputs (Reiterer et al., 2022; Rupp et al., 2023; Reiterer et al., 2023; Bernardini et al., 2024; Lorenzen et al., 2024). For damage diagnosis, signal-processing-based features acting as signal-processing-based damage indices include position-frequency indices formed by CWT coefficient map subtraction between healthy and damaged responses (Bernardini et al., 2021), HHT instantaneous energy profiles (Bernardini et al., 2021), position-dependent RMS profiles and PSD magnitude (Carnevale et al., 2019), and non-symmetric roll-acceleration indices (Bernardini et al., 2020).

Regarding the treatment of EOC variability, only study (Braganca et al., 2024) implements implicit treatment through the PCA models modeling the effects of the varying EOCs, and the residual signal of the PCA models acting as a damage-sensitive feature. Operational variability in the form of speed, axle load, track irregularity, and measurement noise is incorporated in several numerical studies (Carnevale et al., 2019; Bernardini et al., 2020; Bernardini et al., 2021; Braganca et al., 2024; Bernardini et al., 2025a, 2025b), but these parameters are treated as simulation inputs rather than as confounding factors to be explicitly modeled and removed.

3.7. SHM Methods

Using the signal processing techniques and models described in Sections 3.5 and 3.6, the reviewed studies pursue dam-

age diagnosis as the SHM objective, supported by frequency identification that establishes the bridge's baseline dynamic properties.

3.7.1. Frequency identification

Frequency identification supports baseline dynamic characterization by tracking bridge natural frequencies from train-borne measurements. Across all reviewed frequency identification studies (Reiterer et al., 2022; Rupp et al., 2023; Reiterer et al., 2023; Bernardini et al., 2024; Lorenzen et al., 2024; Stour et al., 2025), dominant bending frequencies are recovered from axle-box or bogie acceleration spectra using the methods described in Section 3.5. Changes in the identified frequencies between repeated crossings could, in principle, support damage detection, but none of the reviewed studies implement such a comparison.

3.7.2. Damage diagnosis

Damage diagnosis methods can be grouped into those equipped with data-based models and those that are model-free and rely directly on signal-processing-based features. In both cases, damage is inferred from changes in the damage indices, with the changes being deviations from the baseline.

In the methods equipped with models, the damage indices are model-based damage indices (Bernardini et al., 2025b, 2025a; Braganca et al., 2024) (see the damage indices in Section 3.6). The changes in the indices are expressed via the Mahalanobis distance, in which the damage indices are fused across frequency bands, sensors, and time windows (Braganca et al., 2024) and the Hotelling's T^2 control charts (Bernardini et al., 2025a, 2025b). In study (Bernardini et al., 2025a), damage localization is achieved through multiple segment-specific AENNs that assign statistical deviations to individual bridge segments. Based on these indices, damage detection (Braganca et al., 2024; Bernardini et al., 2025a, 2025b), and localization (Bernardini et al., 2025a) are achieved. In study (Hajializa deh, 2023), the CNNs act as classifiers, and they achieve damage detection, damage localization, and damage quantification (Hajializa deh, 2023).

In studies that do not employ data-based models, damage indices are signal-processing-based, such as CWT coefficients (Bernardini et al., 2021), position-dependent RMS profiles and PSD magnitude (Carnevale et al., 2019), and non-symmetric roll-acceleration signals (Bernardini et al., 2020). These indices support both damage detection (Carnevale et al., 2019; Bernardini et al., 2020; Bernardini et al., 2021) and localization (Carnevale et al., 2019; Bernardini et al., 2020; Bernardini et al., 2021). The peak of the change in CWT coefficients indicates the presence and location of damage, with an alternative HHT-based approach using instantaneous energy (Bernardini et al., 2021). The non-symmetric roll-acceleration signals can indicate damage presence and location without requiring a healthy baseline (Bernardini et al., 2020).

Overall, damage detection is achieved by comparing the damage indices with the baseline phase. Damage localization can be treated as either an estimation problem, where the damage location is inferred from the spatial profile of a continuous index (Carnevale et al., 2019; Bernardini et al., 2020; Bernardini et al., 2021), or a classification problem, where discrete structural segments or prespecified damage states are distinguished (Hajializa deh, 2023; Bernardini et al., 2025a). Also, damage quantification can be treated as a classification problem (Hajializa deh, 2023). No reviewed study achieves damage prognosis within the indirect SHM paradigm for steel railway bridges.

3.8. Strengths and limitations

An overarching practical strength of indirect SHM is that damage indices can be derived from measurements collected on trains during regular service, thereby eliminating the need for permanent sensor installations on every structure in a network. This characteristic offers clear advantages for scalability and cost-efficiency: a single instrumented train can, in principle, survey multiple bridges along a route, whereas direct SHM requires a dedicated installation on each bridge (Carnevale et al., 2019; Reiterer et al., 2022; Bernardini et al., 2025b). The potential for network-level monitoring is further supported by the diversity of technique families demonstrated across the reviewed literature, spanning frequency identification, signal-processing-based damage indices, and data-driven model frameworks, which collectively provide complementary tools for different monitoring objectives.

Within the scope of frequency identification, the evidence base is mature. Several reviewed studies report field campaigns on in-service steel bridges (Rupp et al., 2023; Reiterer et al., 2023; Bernardini et al., 2024; Lorenzen et al., 2024; Stour et al., 2025), covering span lengths from approximately 16 m to 66 m and including both girder and truss bridges. Dominant bending frequencies recovered from axle-box or bogie accelerations show agreement with direct bridge measurements and forced vibration tests (Reiterer et al., 2022; Rupp et al., 2023; Reiterer et al., 2023; Lorenzen et al., 2024; Stour et al., 2025). In (Rupp et al., 2023), the natural frequencies determined from indirect resonance curves match the accuracy of direct measurements, and in (Reiterer et al., 2022), the first longitudinal bending mode is consistently detected in bogie acceleration spectra across multiple crossings. Nevertheless, limitations remain: not all modes are identifiable, with eigenfrequency errors up to 12 % reported in (Stour et al., 2025); reliable identification from bogie responses alone without in-situ benchmarks remains challenging (Reiterer et al., 2023); amplitude-dependent frequency behavior (Lorenzen et al., 2024) and the influence of track irregularity (Bernardini et al., 2024) require further refinement; and generalization across

diverse bridge types and operational envelopes has not been systematically assessed.

For damage diagnosis, several studies demonstrate detection and, in selected cases, localization and quantification using signal-processing-based and model-based damage indices (Carnevale et al., 2019; Bernardini et al., 2020; Bernardini et al., 2021; Braganca et al., 2024; Bernardini et al., 2025a, 2025b). Methodological strengths include robustness testing under operational variability – incorporating speed variation, track irregularity profiles, and measurement noise (Bernardini et al., 2020; Bernardini et al., 2021; Braganca et al., 2024; Bernardini et al., 2025a, 2025b) – and the use of batch processing and multi-source data fusion to stabilize damage indicators across repeated crossings (Braganca et al., 2024; Bernardini et al., 2025a, 2025b). Under favorable conditions, reported damage detection performance is high, with damage detected at stiffness reductions as low as 1 % (Braganca et al., 2024) and accurate damage localization achieved using multi-sensor configurations (Bernardini et al., 2025a) or baseline-free roll-acceleration analysis (Bernardini et al., 2020). The supervised CNN framework in (Hajializa deh, 2023) achieves 100 % accuracy in damage detection, localization, and quantification on unseen test data, although this result is obtained on a scaled laboratory bridge.

Despite these methodological advances, significant limitations constrain the current readiness of indirect SHM for operational deployment. The most critical gap is the reliance on numerical simulations for damage diagnosis. Of the studies targeting damage diagnosis, six are validated exclusively through numerical vehicle-track-bridge interaction models (Carnevale et al., 2019; Bernardini et al., 2020; Bernardini et al., 2021; Braganca et al., 2024; Bernardini et al., 2025a, 2025b), and only (Hajializa deh, 2023) presents experimental results on a 2.56 m scaled laboratory bridge with damage simulated via added masses. No reviewed study reports field validation of damage detection on an in-service steel railway bridge with confirmed structural damage.

Further limitations are evident across several dimensions. Detection of low-severity damage remains a challenge: in (Bernardini et al., 2025b), the lightest cross-girder damage (15 % stiffness reduction) requires 40 train passages to achieve 100 % accuracy, sensitivity to corrosion below 10 % is low in study (Bernardini et al., 2025a), and the overall result quality under changing track-irregularity profiles is moderate in study (Bernardini et al., 2021). Environmental variability receives minimal attention, with study (Braganca et al., 2024) incorporating temperature effects indirectly through variation in material stiffness, while the remaining studies either neglect environmental factors or conduct field tests under ambient conditions without explicit mitigation (Reiterer et al., 2022; Rupp et al., 2023; Reiterer et al., 2023; Lorenzen et al., 2024; Stour et al., 2025). The reviewed studies also predominantly consider Warren-type trusses (Bernardini et al., 2025b, 2021, 2025a; Braganca et al., 2024; Bernardini et al., 2020, 2024; Stour et al., 2025) and short-to medium-span girder bridges (Carnevale et al., 2019; Reiterer et al., 2022; Rupp et al., 2023; Reiterer et al., 2023; Lorenzen et al., 2024), with only one study achieving damage quantification (Hajializa deh, 2023), and no study achieving damage prognosis.

Table 4 presents a summary of the main information about the indirect frequency identification and SHM studies.

4. FUTURE DIRECTIONS

Based on the research gaps identified across the reviewed direct and indirect SHM studies on steel railway bridges, the following directions are considered most critical for advancing the field toward operational deployment.

- **Field validation with confirmed damage data.** This is the most frequently cited gap across the reviewed literature. For direct SHM, many diagnostic methods are validated using FEM-generated damage scenarios or retrofitting data that may not reflect actual damage behavior, whereas most of the reviewed field studies use no decision threshold for damage diagnosis. For indirect SHM, no study reports field validation of damage detection on an in-service steel railway bridge with confirmed structural damage. Field validation on real bridges with confirmed damage states, as recommended by the majority of the reviewed studies, would substantially strengthen the evidence base for both approaches.
- **Environmental and operational variability.** Inadequate treatment of EOCs is identified as a limitation across both direct and indirect studies. Among the direct SHM studies, the effects of EOC changes are not considered in most of the reviewed field studies, and the influence of temperature, wind, and seasonal changes on damage indices remains poorly characterized. Among the indirect SHM studies, only study (Braganca et al., 2024) implements an implicit variability treatment via PCA models, with temperature modeled as a function of material stiffness variation. Systematic incorporation of EOC effects through data normalization, implicit modeling, and improved separation of EOC-induced variability from damage-related changes is essential for enabling reliable damage detection under realistic EOCs.
- **Method robustness, generalization, and decision thresholds.** A substantial number of the reviewed studies recommend improvements in method robustness. Recurring challenges include low sensitivity to mild damage in both direct (Rageh et al., 2018; Anastasia et al., 2023) and indirect (Bernardini et al., 2025a, 2025b) approaches, absence of standardized decision thresholds, and performance degradation with reduced sensor networks (Beskhyroun et al., 2010, 2012; Oshima et al., 2013; Chen et al., 2014;

Table 4. Review of studies about indirect frequency identification and SHM in railway bridges.

Reference	Bridge type	Damage type	Sensor type	Validation type	Environmental variable	Operational variable	Data processing	Modeling	SHM method	Objective
(Reiterer et al., 2023)	Girder	-	Accelerometers	Field	-	-	Low-pass filtering, FFT spectrum-based OMA	-	-	Frequency identification
(Rupp et al., 2023)	Girder	-	Accelerometers, strain gauges, velocimeters, thermocouples, displacement sensors	Field	-	-	Butterworth low-pass filtering, SSI-based OMA	State space models	-	Frequency identification
(Bernardini et al., 2024)	Truss	-	Accelerometers	Field	-	-	Low-pass filtering, FFT spectrum-based OMA	-	-	Frequency identification
(Stour et al., 2025)	Truss	-	Accelerometers	Field	-	-	SSI-Cov-based OMA, ARMAX model-based OMA, DKF framework	State space models, ARMAX models	-	Frequency identification
(Lorenzen et al., 2024)	Beam	-	Accelerometers	Field	-	-	FFT-based OMA	-	-	Frequency identification

Table 4. Cont.

Reference	Bridge type	Damage type	Sensor type	Validation type	Environmental variable	Operational variable	Data processing	Modeling	SHM method	Objective
(Reiterer et al., 2022)	Girder	-	Accelerometers	Field, numerical	-	Train speed	Low-pass filtering, FFT spectrum-based OMA	-	-	Frequency identification
(Bernardini et al., 2025b)	Truss	Corrosion simulated by elasticity modulus & material density & stiffness reduction	Accelerometers, velocimeters	Numerical	-	Number of train passages, axle load, train speed	CWT with complex Morlet wavelets	AENNs	Changes in reconstruction error from AENNs expressed via the Hotelling's T^2 control charts	Damage detection
(Bernardini et al., 2021)	Truss	Loosen bolts or cracked welds simulated via elasticity modulus reduction	Accelerometers, velocimeters	Numerical	-	Train speed	CWT with complex Morlet wavelets, HHT	-	Changes in CWT coefficients	Damage detection, localization
(Carnevale et al., 2019)	Beam	Stiffness reduction	Accelerometers	Numerical	-	Train speed	Quasi-static component isolation via low-pass filtering combined with moving-window RMS computation	-	Changes in position-dependent RMS profiles & PSD magnitude	Damage detection, localization

Table 4. Cont.

Reference	**Bridge type**	**Damage type**	**Sensor type**	**Validation type**	**Environmental variable**	**Operational variable**	**Data processing**	**Modeling**	**SHM method**	**Objective**
(Bernardini et al., 2025a)	Truss	Corrosion simulated via elasticity modulus, material density, stiffness reduction	Accelerometers	Field, numerical	-	Number of train passages, axle load, train speed	CWT with complex Morlet wavelets	AENNs	Changes in reconstruction error from AENNs expressed via the Hotelling's T^2 control charts	Damage detection, localization
(Hajializadeh, 2023)	Beam	Added mass	Accelerometers	Experimental	-	Train speed	STFT	CNNs	CNNs acting as classifiers	Damage detection, localization, quantification
(Braganca et al., 2024)	Truss	Stiffness reduction	Accelerometers	Numerical	-	Axle load, train speed	Chebyshev II low-pass filtering, WST	AENNs, PCA models	Changes in residual signal of PCA models expressed via the Mahalanobis distance	Damage detection
(Bernardini et al., 2020)	Truss	Loosen bolts or cracked welds simulated via stiffness reduction	Accelerometers	Numerical	-	Train speed	Low-pass Butterworth filtering, roll-acceleration differencing	-	Changes in non-symmetric roll-acceleration signals	Damage detection, localization

Rageh et al., 2018; Zhang et al., 2019; Li et al., 2022; Svendsen et al., 2022, 2023; Anastasia et al., 2023; Quqa et al., 2024; Monti et al., 2025). Future work should address the definition of operational decision limits, sensor placement optimization for cost-effective deployment, and the development of adaptive baselines that can evolve after confirmed structural changes.

- **Advancing damage quantification and prognosis.** For direct SHM, damage quantification is achieved in several studies but is treated predominantly as a classification task, and prognosis is limited to component-level fatigue assessment via CDM-based and FM-based methods (Leander et al., 2010; Siriwardane et al., 2010; Tochaei et al., 2021; Zakharenko et al., 2022; Sangiorgio et al., 2022) rather than system-level RUL estimation (Tochaei et al., 2021). For indirect SHM, no reviewed study achieves damage prognosis, and only one study achieves damage quantification (Hajializa deh, 2023). Bridging this gap will require extending indirect SHM from detection toward damage quantification, and RUL estimation (Hajializa deh, 2023; Braganca et al., 2024), and integrating monitoring outputs with prognosis models to support condition-based maintenance decisions (Leander et al., 2010; Siriwardane et al., 2010; Tochaei et al., 2021; Zakharenko et al., 2022; Sangiorgio et al., 2022).

  Bridging frequency identification to damage detection. The reviewed indirect SHM studies on frequency identification recover bridge natural frequencies from train-borne sensors but stop short of damage detection (Reiterer et al., 2022; Rupp et al., 2023; Reiterer et al., 2023; Bernardini et al., 2024; Lorenzen et al., 2024; Stour et al., 2025). Future work should establish baseline-comparison and threshold-decision frameworks that translate frequency identification outputs into operational damage indicators, including the explicit treatment of EOC-induced frequency drift and amplitude-dependent frequency behavior (Lorenzen et al., 2024; Bernardini et al., 2024), so that the maturity already achieved in frequency identification can be carried forward into the SHM workflow.

Other directions raised by the reviewed studies include broadening the scope to bridge types beyond Warren trusses and short-to-medium-span girders, including different geometries, materials, and multi-span configurations (Bernardini et al., 2020; Hajializa deh, 2023; Braganca et al., 2024; Bernardini et al., 2025a), assessing performance under combined multi-damage scenarios, and optimizing train-mounted sensor configurations for indirect monitoring (Rupp et al., 2023).

Looking ahead, emerging technologies may offer pathways to address several of the above gaps simultaneously. Digital twin frameworks that couple calibrated physics-based models with continuously updated field data could support both real-time damage diagnosis and damage prognosis. Physics-informed machine learning may improve generalization under limited field data by embedding structural mechanics constraints into data-driven architectures. Complementary inspection modalities, including Unmanned Aerial Vehicle (UAV)-based monitoring, could augment vibration-based SHM by providing additional condition information beyond dynamic response data. The integration of these paradigms within intelligent transportation systems and smart infrastructure management platforms represents a promising direction for achieving scalable, lifecycle-oriented SHM of steel railway bridge networks.

The monitoring objectives, damage detection, localization, quantification, and RUL estimation, reviewed in this paper, are most valuable when they are explicitly connected to maintenance decision-making frameworks. From a Prognostics and Health Management (PHM) perspective, the outputs of SHM systems should inform condition-based maintenance strategies, in which inspection and intervention decisions are triggered by the current structural state rather than fixed time intervals. This requires not only accurate damage indicators but also principled uncertainty quantification, accounting for both aleatory uncertainties (load variability, material scatter, environmental fluctuations) and epistemic uncertainties (model errors, limited training data, sensor noise) to deliver actionable, grounded RUL estimates. Risk-based inspection frameworks can then use these estimates to prioritize interventions across a bridge network by allocating resources to locations where the probability of failure and the consequences of failure jointly exceed an acceptable threshold. The combined direct/indirect deployment strategy proposed in the conclusions maps naturally onto this framework: indirect train-borne monitoring provides a continuous, low-cost network-level screening layer that updates the risk ranking of all the bridges of a railway line, while direct sensor installations are reserved for bridges flagged as high-risk, where higher-resolution condition assessment and RUL estimation are required to support maintenance planning. Realizing this vision requires closer integration between the SHM research community and asset management practice, including the adoption of standardized decision thresholds, digital twin architectures capable of assimilating monitoring data in near real time, and lifecycle cost models that can quantify the economic value of the monitoring information itself.

5. CONCLUSIONS

This review has examined the state-of-the-art on vibration-based direct and indirect SHM in steel railway bridges between 2010 and 2025, covering 32 studies about direct SHM and 13 studies about indirect SHM. Direct SHM has matured, with a well-validated framework demonstrated on real bridges of various types and lengths, achieving low misclassification rates in many studies. Indirect SHM, while considerably less mature, has demonstrated meaningful progress since its first application to steel railway bridges in 2019. The 6 frequency identification studies confirm that train-borne accelerometers

can extract bridge natural frequencies, while the 7 damage diagnosis studies achieve damage detection and, in selected cases, localization and quantification. Despite these advances, both approaches share critical limitations.

The most important insight emerging from this review is that direct and indirect SHM are not competing but complementary approaches, whose integration represents the most promising pathway toward reliable, scalable, and cost-effective monitoring of steel railway bridge networks. From a PHM standpoint, this integration should be understood as a two-tier condition-based maintenance architecture. Instrumented trains performing routine network-level monitoring generate a continuously updated risk ranking across all the bridges of a railway line, thus enabling risk-based prioritization of inspection and maintenance resources. Bridge-mounted sensors, reserved for bridges flagged as high-risk, provide the higher-resolution structural state assessment and RUL estimates needed to support maintenance intervention decisions under uncertainty. This strategy would also allow indirect monitoring results to be validated against direct measurements on the same structures, thus addressing the field-validation gap that currently limits the operational readiness of indirect SHM. Achieving this vision will require sustained progress on the limitations identified in this review.

ACKNOWLEDGMENT

Funded by the European Union. Views and opinion expressed are however those of the author(s) only and do not necessarily reflect those of the European Union or Europe's Rail Joint Undertaking. Neither the European Union nor the granting authority can be held responsible for them. The project is supported by the Europe's Rail Joint Undertaking and its members. This project has received funding from the European Union's Horizon Europe research and innovation programme under Grant Agreement No. 101101966.

REFERENCES

Anastasia, S., Garcia-Macias, E., Ubertini, F., Gattulli, V., & Ivorra, S. (2023). Damage identification of railway bridges through temporal Autoregressive modeling. *Sensors*, *23*, 8830.

Anastasopoulos, D., & Reynders, E. P. B. (2023). Modal strain monitoring of the old Nieuwebrugstraat bridge: Local damage versus temperature effects. *Engineering Structures*, *296*, 116854.

Armijo, A., & Zamora-Sanchez, D. (2024). Integration of railway bridge structural health monitoring into the internet of things with a digital twin: A case study. *Sensors*, *24*, 2115.

Azim, M., & Gul, M. (2021). Data-driven damage identification technique for steel truss railroad bridges utilizing principal component analysis of strain response. *Structure and Infrastructure Engineering: Maintenance, Management, Life-Cycle Design and Performance*, *17*(8), 1019–1035.

Bernardini, L., Bono, F. M., & Collina, A. (2025a). Drive-by damage detection and localization exploiting continuous wavelet transform and multiple sparse autoencoders. *Railway Engineering Science*, *33*, 721–745.

Bernardini, L., Bono, F. M., & Collina, A. (2025b). Drive-by damage detection based on the use of CWT and sparse autoencoder applied to steel truss railway bridge. *Advances in Mechanical Engineering*, *17*(5), 16878132251339857.

Bernardini, L., Carnevale, M., & Collina, A. (2021). Damage identification in warren truss bridges by two different time–frequency algorithms. *Applied Sciences*, *11*, 10605.

Bernardini, L., Carnevale, M., Somaschini, C., Matsuoka, K., & Collina, A. (2020). A numerical investigation of new algorithms for the drive-by method in railway bridge monitoring. In *Proceedings of the 11th international conference on structural dynamics (eurodyn)* (pp. 1033–1043). Athens, Greece.

Bernardini, L., Matsuoka, K., & Collina, A. (2024). Indirect frequency estimation by time-shifted accelerations subtraction: Generalization of the methodology and numerical application on a Warren truss bridge. *Journal of Sound and Vibration*, *590*, 118491.

Beskhyroun, S., Oshima, T., & Mikami, S. (2010). Wavelet-based technique for structural damage detection. *Structural Control and Health Monitoring*, *17*, 473–494.

Beskhyroun, S., Wegner, L. D., & Sparling, B. F. (2012). New methodology for the application of vibration-based damage detection techniques. *Structural Control and Health Monitoring*, *19*, 632–649.

Braganca, C., Souza, D., E. F .and Ribeiro, & Bittencourt, T. (2024). Drive-by early damage detection in railway bridges using wavelets and autoencoders. In *Proceedings of the 6th international conference on railway technology: Research, development and maintenance (railways)* (Vol. 15). Prague, Czech Republic.

Carnevale, M., Collina, A., & Peirlinck, T. (2019). A feasibility study of the drive-by method for damage detection in railway bridges. *Applied Sciences*, *9*, 160.

Chen, Z. W., Zhu, S., Xu, Y. L., Li, Q., & Cai, Q. L. (2014). Damage detection in long suspension bridges using stress influence lines. *Journal of Bridge Engineering*, *20*.

Corbally, R., & Malekjafarian, A. (2023). Detecting changes in the structural behaviour of a laboratory bridge model using the contact-point response of a passing vehicle. *Journal of Structural Integrity and Maintenance*, *8*, 226–238.

Dang, H. V., Tatipamula, M., & Nguyen, H. X. (2022). Cloud-based digital twinning for structural health monitoring using deep learning. *IEEE Transactions on Industrial Informatics*, *18*(6), 3820–3830.

Froseth, G. T., Ronnquist, A., Cantero, D., & Oiseth, O. (2017). Influence line extraction by deconvolution in the frequency domain. *Computers and Structures*, *189*, 21–30.

Frøseth, G., & Rönnquist, A. (2019). Load model of historic traffic for fatigue life estimation of norwegian railway bridges. *Engineering Structures*, *200*, 109626.

Ghiasi, A., Moghadda, M. K., Ng, C. T., Sheikh, A. H., & Shi, J. Q. (2022). Damage classification of in-service steel railway bridges using a novel vibration-based convolutional neural network. *Engineering Structures*, *264*, 114474.

Ghiasi, A., Ng, C. T., & Sheikh, A. H. (2022). Damage detection of in-service steel railway bridges using a fine k-nearest neighbor machine learning classifier. *Structures*, *45*, 1920–1935.

Guo, W. C., Orcesi, A. D., Cremona, C. F., Santos, J. P., Yang, S. Z., & L., D. (2012). A vibration-based framework for structural health monitoring of railway bridges. In *Proceedings of the 3rd international symposium on life cycle civil engineering (ialcce).* Vienna, Austria.

Hajializa deh, D. (2023). Deep learning-based indirect bridge damage identification system. *Structural Health Monitoring*, *22*(2), 897–912.

Imam, B. M., & Chryssanthopoulos, M. K. (2012). Causes and consequences of metallic bridge failures. *Structural Health Monitoring*, *22*(1), 93–98.

Leander, J., Andersson, A., & Karoumia, R. (2010). Monitoring and enhanced fatigue evaluation of a steel railway bridge. *Engineering Structures*, *32*(3), 854-863.

Lee, J. S., Park, J., Kim, H. M., & Kim, R. E. (2024). Damage detection for railway bridges using time-frequency decomposition and conditional generative model. *Computer-Aided Civil and Infrastructure Engineering*, *40*, 959–977.

Li, Y., Ding, Y., Zhao, H., & Sun, Z. (2022). Data-driven structural condition assessment for high-speed railway bridges using multi-band FIR filtering and clustering. *Structures*, *41*, 1546–1558.

Lorenzen, S. R., Rupp, M. M., & Hubler, C. (2024). Frequency identification using resonance curve-based drive-by monitoring: Field validation. In *Proceedings of the 10th european workshop on structural health monitoring (ewshm).* Potsdam, Germany.

Maes, K., Meerbeeck, L. V., Reynders, E. P. B., & Lombaert, G. (2022). Validation of vibration-based structural health monitoring on retrofitted railway bridge KW51. *Mechanical Systems and Signal Processing*, *165*, 108380.

Malekjafarian, A., McGetrick, P. J., & OBrien, E. J. (2015). A review of indirect bridge monitoring using passing vehicles. *Shock and Vibration*, *2015*.

Menghini, A., Leander, J., & Castiglioni, C. A. (2023). A local response function approach for the stress investigation of a centenarian steel railway bridge. *Engineering Structures*, *286*, 116116.

Monti, G., Rabi, R. R., Marella, L., & Proietti, S. T. (2025). Data-driven decision support system for the safety management of railway bridge networks. *Reliability Engineering and System Safety*, *262*, 111202.

Neves, A. C., Gonzalez, I., & Karoumi, R. (2022). Development and validation of a data-based shm method for railway bridges. In A. Cury, D. Ribeiro, F. Ubertini, & M. D. Todd (Eds.), *Structural integrity:structural health monitoring based on data science techniques* (Vol. 21, pp. 95–116). New York: Springer.

Nguyen, D. C., Salamak, M., Katunin, A., Poprawa, G., Przystalka, P., & Hypki, M. (2024). Vibration-based shm of debica railway steel bridge with optimized ann and anfis. *Journal of Constructional Steel Research*, *215*, 108505.

Oshima, T., Miyamori, Y., Mikami, S., Yamazaki, T., Beskhyroun, S., & Kopacz, M. F. (2013). Small damage detection of real steel bridge by using local excitation method. *Journal of Civil Structural Health Monitoring*, *3*, 307–315.

Pourtarki, A., Ghavifekr, H. B., & Afshin, H. (2023). Study

on the dynamic behaviour of Bafgh-Bandar Abbas lane railway bridge for structural health monitoring purpose. *Australian Journal of Structural Engineering*, *24*, 243–253.

Quqa, S., Palermo, A., & Marzani, A. (2024). Damage index based on the strain-to-displacement relation for health monitoring of railway bridges. *Computer-Aided Civil and Infrastructure Engineering*, *39*, 3145–3163.

Rageh, A., Linzell, D. G., & E., A. S. (2018). Automated, strain-based, output-only bridge damage detection. *Journal of Civil Structural Health Monitoring*, *8*, 833–846.

Reiterer, M., Bettinelli, L., Schellander, J., Stollwitzer, A., & Fink, J. (2023). Application of vehicle-based indirect structural health monitoring method to railway bridges—simulation and in monitoring method to railway bridges-simulation and in situ test. *Applied Sciences*, *13*, 10928.

Reiterer, M., Bettinelli, L., Stollwitzer, A., Schellander, J., & Fink, J. (2022). Vehicle-based indirect SHM of an Austrian railway bridge: Simulation and in-situ test. In P. Rizzo & A. Milazzo (Eds.), *Lecture notes in civil engineering: European workshop on structural health monitoring (ewshm) - volume 1* (Vol. 253, pp. 721–731). Switzerland: Springer.

Rupp, M. M., Lorenzen, S. R., Fritzsche, M. A., Riedel, H., Kohl, A., Apostolidi, E., & Schneider, J. (2023). High-speed drive-by monitoring: field testing with an intercity express train (ICE). *Applied Sciences*, *6*, 854–862.

Sangiorgio, V., Nettis, A., Uva, G., Pellegrino, F., Varum, H., & Adam, J. M. (2022). Analytical fault tree and diagnostic aids for the preservation of historical steel truss bridges. *Engineering Failure Analysis*, *133*, 105996.

Sarmadi, H., Entezami, A., Behkamal, B., & Michele, C. (2022). Partially online damage detection using long-term modal data under severe environmental effects by unsupervised feature selection and local metric learning. *Journal of Civil Structural Health Monitoring*, *12*, 1043–1066.

Siriwardane, S. A. S. C., Ohga, M., Dissanayake, P. B. R., & Kaita, T. (2010). Structural appraisal-based different approach to estimate the remaining fatigue life of railway bridges. *Structural Health Monitoring*, *9*(4), 323–339.

Stour, C. D., Gres, S., Dertimanis, V. K., Ancu, L., & Chatzi, E. N. (2025). Identification of railway bridge modal properties based solely on acceleration data from traversing trains. *Mechanical Systems and Signal Processing*, *239*, 113342.

Svendsen, B. T., Froseth, G. T., Oiseth, O., & Ronnquist, A. (2022). A data-based structural health monitoring approach for damage detection in steel bridges using experimental data. *Journal of Civil Structural Health Monitoring*, *12*, 101–115.

Svendsen, B. T., Oiseth, O., Froseth, G. T., & Ronnquist, A. (2023). A hybrid structural health monitoring approach for damage detection in steel bridges under simulated environmental conditions using numerical and experimental data. *Structural Health Monitoring*, *22*(1), 540–561.

Tochaei, E. N., Fang, Z., Taylor, T., Babanajad, S., & Ansari, F. (2021). Structural monitoring and remaining fatigue life estimation of typical welded crack details in the manhattan bridge. *Engineering Structures*, *231*, 111760.

Torres, B., Poveda, P., Ivorra, S., & Estevan, L. (2023). Long-term static and dynamic monitoring to failure scenarios assessment in steel truss railway bridges: A case study. *Engineering Failure Analysis*, *152*, 107435.

Vagnoli, M., Remenyte-Prescott, R., & Andrews, J. (2017). Railway bridge structural health monitoring and fault detection: State-of-the-art methods and future challenges. *Structural Health Monitoring*, *17*, 971–1007.

Wang, Y. W., Ni, Y.-Q., & Wang, S. M. (2022). Structural health monitoring of railway bridges using innovative sensing technologies and machine learning algorithms: a concise review. *Intelligent Transportation Infrastructure*, *1*, liac009.

Yano, M. O., Figueiredo, E., Silva, S. D., Cury, A., & Moldovan, I. (2023). Transfer learning for structural health monitoring in bridges that underwent retrofitting. *Buildings*, *13*(9), 2323.

Ye, X., Su, Y., & Han, J. (2014). A state-of-the-art review on fatigue life assessment of steel bridges. *Mathematical Problems in Engineering*, *2014*, 956473.

Zakharenko, M., Frøseth, G. T., & Ronnquist, A. (2022). How conservative is the Norwegian fatigue load model for service life estimation of railway bridges? *Structure and Infastracture Enginnering*, *20*, 1404–1417.

Zhang, Y., Miyamori, S., Y.and Mikami, & Saito, T. (2019). Vibration-based structural state identification by a 1-dimensional convolutional neural network. *Computer-Aided Civil and Infrastructure Engineering*, *34*, 822–

839.

BIOGRAPHIES

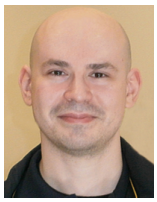

Dr. Christos Sakaris works as a Researcher in the DARWIN research group of NORCE Research AS. He received his Diploma (combination of a bachelor's degree and a master's degree) in Mechanical Engineering from Aristotle University of Thessaloniki, Greece (2009), and his PhD in Mechanical and Aeronautical Engineering from the University of Patras, Greece (2018). Dr. Sakaris has worked as a Postdoctoral Research Fellow in the Liverpool Logistics, Offshore and Marine (LOOM) Research Institute of Liverpool John Moores University, United Kingdom, and as a Postdoctoral Researcher in NORCE Research AS. He has participated in various national projects, including AIMWind, RIWUP, SusOffAqua, and the EU projects ARCWIND (Adaptation and implementation of floating wind energy conversion technology for the Atlantic Region), STORHY (innovative hydropower storage technology and operations), and IAM4RAIL (holistic and integrated asset management for Europe's rail system). His research interests include vibration-based diagnosis and prognosis using machine learning methods, structural / modal analysis via data-based statistical models, signal processing, and SHM for bridges, floating offshore wind turbines, fish farms, and wooden structures.

Dr. Zihao Liu works as a Research Assistant in the University of New South Wales (UNSW), School of Civil and Environmental Engineering, Australia. Dr. Liu holds a bachelor's degree in Civil Engineering from Central South University, Changsha, China (2018), a master's degree in Civil Engineering from the University of Sydney, Sydney, Australia (2021), and a PhD in Structural Engineering from the University of Sydney, Sydney, Australia (2025).

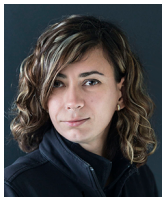

Dr. Mehrisadat Makki Alamdari works as a Senior Lecturer at the University of New South Wales (UNSW), School of Civil and Environmental Engineering, Australia. Dr. Alamdari holds a bachelor's degree in Aerospace Engineering from Sharif University of Technology, Tehran, Iran (2006), a master's degree in Aerospace Engineering from Iran University of Science and Technology, Tehran, Iran (2008), a master's degree in Mechanical Engineering from the University of Manitoba, Winnipeg, Canada (2011) and a PhD in Civil Engineering from the University of Technology, Sydney, Australia (2014). Prior to joining UNSW, she was a research fellow in Data61—CSIRO. She is the recipient of the highly competitive ARC Discovery Early Career Research Award (DECRA). Dr. Alamdari is also the winner of the prestigious JSPS Award (Japan Society for Promotion of Science). An award-winning scholar, Mehri is on the Executive of the Australian Network of Structural Health Monitoring (ANSHM), a member of the International Society for Structural Health Monitoring of Intelligent Infrastructure (ISHMII), a member of the International Association for Bridge Maintenance and Safety (IABMAS), and a steering committee member in Australia, New Zealand and Oceania Researchers in Japan Network (ANZOR Japan Network). Dr. Alamdari has contributed to the development and deployment of SHM systems for several large-scale bridges, including the iconic Sydney Harbour Bridge in Sydney, and the Gateway Bridge in Brisbane. For these contributions, she and her team have been awarded Intelligent Transport Systems (ITS) Australia National Awards in 2020 and the Most Practical SHM Solutions for Civil / Mechanical Systems Award from Stanford University in 2015. Dr. Alamdari's expertise is vibration analysis and testing, inverse dynamic problems, and signal processing. She is an Editor of the International Measurement Confederation (IMEKO) [Elsevier]. Her interests include Structural Health Monitoring, vibration analysis and testing, inverse dynamic problems, signal processing, and data mining.

Dr. Rune Schlanbusch works as Chief Scientist and Deputy Head of the DARWIN research group of NORCE Research AS, Norway. Dr. Schlanbusch holds a master's degree in Space Technology from Narvik University College (now University in Tromso - The Arctic University of Norway), Narvik, Norway (2007), and a PhD in Engineering Cybernetics from Norwegian University of Science and Technology (NTNU), Trondheim, Norway (2010). Dr. Schlanbusch has served as Chief Technology Officer for the spin-off company Machine Prognostics. He has participated in several major national and international research projects and research centers, including the Centers for Research-Driven Innovation (SFI) Offshore Mechatronics, the IKTPluss projects AIMWind, PHMHydro, SusOffAqua, the capacity-building project ImpactWind, the Green Platform project for optimizing maintenance and repair of floating offshore wind turbines, and the EU projects STORHY and IAM4RAIL. Dr. Schlanbusch contributes as an expert in condition monitoring in the International Energy Agency (IEA) Wind Task 49 Reference Floating Wind Array Design Basis, serves on the management committee of the COST Action Pan-European Network for Sustainable Hydropower, and holds coordination responsibility for offshore wind in the Energy and Technology division at NORCE. He is a member of IEEE, and his daily work focuses on condition monitoring of machines, equipment, and infrastructure through developing new sensor technologies, monitoring and inspection systems, control systems, and robotic solutions to improve operations and maintenance.